The Src family kinases Hck, Fgr, and Lyn are critical for the generation of the in vivo inflammatory environment without a direct role in leukocyte recruitment

Miklós Kovács,[1,2] Tamás Németh,[1,2] Zoltán Jakus,[1,3] Cassian Sitaru,[4] Edina Simon,[1,2] Krisztina Futosi,[1] Bálint Botz,[5,6] Zsuzsanna Helyes,[5,6] Clifford A. Lowell,[7] and Attila Mócsai[1,2]

[1]Department of Physiology, Semmelweis University School of Medicine, 1094 Budapest, Hungary
[2]MTA-SE "Lendület" Inflammation Physiology Research Group of the Hungarian Academy of Sciences and the Semmelweis University, and [3]MTA-SE "Lendület" Lymphatic Physiology Research Group of the Hungarian Academy of Sciences and the Semmelweis University, 1094 Budapest, Hungary
[4]Department of Dermatology, University Hospital Freiburg and BIOSS Centre for Biological Signalling Studies, 79104 Freiburg, Germany
[5]Department of Pharmacology and Pharmacotherapy, Faculty of Medicine, and [6]János Szentágothai Research Centre, University of Pécs, 7624 Pécs, Hungary
[7]Department of Laboratory Medicine, University of California, San Francisco, San Francisco, CA 94143

Although Src family kinases participate in leukocyte function in vitro, such as integrin signal transduction, their role in inflammation in vivo is poorly understood. We show that Src family kinases play a critical role in myeloid cell–mediated in vivo inflammatory reactions. Mice lacking the Src family kinases Hck, Fgr, and Lyn in the hematopoietic compartment were completely protected from autoantibody-induced arthritis and skin blistering disease, as well as from the reverse passive Arthus reaction, with functional overlap between the three kinases. Though the overall phenotype resembled the leukocyte recruitment defect observed in β_2 integrin–deficient (CD18$^{-/-}$) mice, Hck$^{-/-}$Fgr$^{-/-}$Lyn$^{-/-}$ neutrophils and monocytes/macrophages had no cell-autonomous in vivo or in vitro migration defect. Instead, Src family kinases were required for the generation of the inflammatory environment in vivo and for the release of proinflammatory mediators from neutrophils and macrophages in vitro, likely due to their role in Fcγ receptor signal transduction. Our results suggest that infiltrating myeloid cells release proinflammatory chemokine, cytokine, and lipid mediators that attract further neutrophils and monocytes from the circulation in a CD18-dependent manner. Src family kinases are required for the generation of the inflammatory environment but not for the intrinsic migratory ability of myeloid cells.

CORRESPONDENCE
Attila Mócsai:
mocsai.attila@
med.semmelweis-univ.hu

Abbreviations used: FcRγ, Fc receptor γ-chain; GST, glutathione S-transferase; ITAM, immunoreceptor tyrosine-based activation motif; KC, keratinocyte chemoattractant; LTB_4, leukotriene B_4; MCP-1, monocyte chemoattractant protein 1; MIP-2, macrophage inflammatory protein 2; MPO, myeloperoxidase; ROS, reactive oxygen species.

Src family kinases are best known for their role in malignant transformation and tumor progression, as well as signaling through cell surface integrins (Parsons and Parsons, 2004; Playford and Schaller, 2004). Due to their role in cancer development and progression, Src family kinases have become major targets of cancer therapy (Kim et al., 2009; Zhang and Yu, 2012). Src family kinases are also present in immune cells with dominant expression of Lck and Fyn in T cells and NK cells; Lyn, Fyn, and Blk in B cells and mast cells; and Hck, Fgr, and Lyn in myeloid cells such as neutrophils and macrophages (Lowell, 2004).

The best known function of Src family kinases in the immune system is their role in integrin signal transduction. Indeed, Hck, Fgr, and Lyn mediate outside-in signaling by β_1 and β_2 integrins in neutrophils and macrophages (Lowell et al., 1996; Meng and Lowell, 1998; Mócsai et al., 1999; Suen et al., 1999; Pereira et al., 2001; Giagulli et al., 2006; Hirahashi et al., 2006), Lck participates in LFA-1–mediated T cell responses (Morgan et al., 2001; Fagerholm et al., 2002; Feigelson et al., 2001; Suzuki et al., 2007), and Src family kinases are required for LFA-1–mediated

The Rockefeller University Press $30.00
J. Exp. Med. 2014 Vol. 211 No. 10 1993-2011
www.jem.org/cgi/doi/10.1084/jem.20132496

The Journal of Experimental Medicine

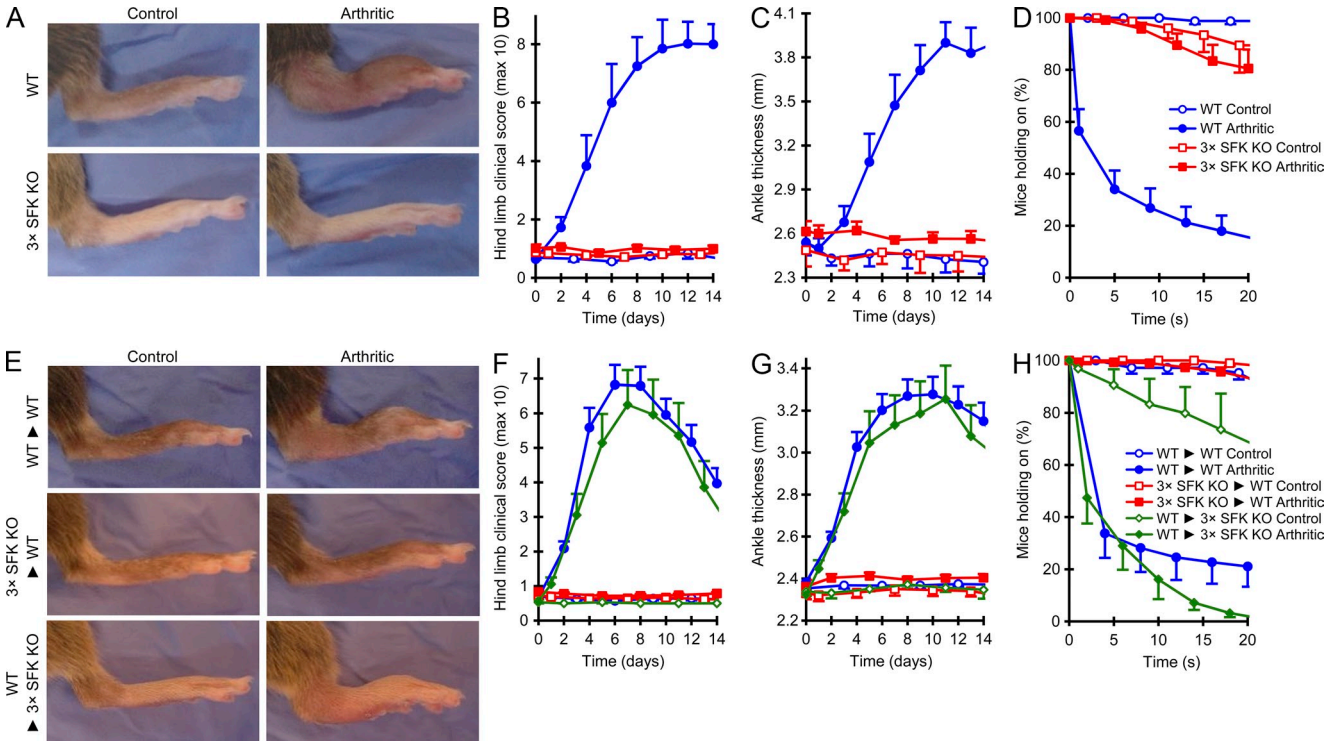

Figure 1. Myeloid Src family kinases are indispensable for autoantibody-induced arthritis. Intact (A–D) WT or Hck$^{-/-}$Fgr$^{-/-}$Lyn$^{-/-}$ (3× SFK KO) mice or bone marrow chimeras (E–H) generated by transplanting WT or Hck$^{-/-}$Fgr$^{-/-}$Lyn$^{-/-}$ bone marrow to WT (WT▶WT and 3× SFK KO▶WT, respectively) or Hck$^{-/-}$Fgr$^{-/-}$Lyn$^{-/-}$ recipients (WT▶3× SFK KO) were injected with B×N (control) or K/B×N (arthritic) serum i.p. on day 0. Arthritis development was followed by photographing on day 8 (A and E), clinical scoring of the hind limbs (B and F), ankle thickness measurement (C and G) and an articular function test (hanging on a wire grid; D and H). Images are representative of, and quantitative data show mean and SEM from, 4 control and 6 arthritic serum-treated individual mice per group from 2 independent experiments (A–D) or 4–12 control and 7–26 arthritic serum-treated mice per group from 2–8 independent experiments (E–H). D and H show results from functional test performed 6–21 times on each mouse between days 6–12.

signal transduction and target cell killing by NK cells (Riteau et al., 2003; Perez et al., 2004).

Src family kinases also mediate TCR signal transduction by phosphorylating the TCR-associated immunoreceptor tyrosine-based activation motifs (ITAMs), leading to recruitment and activation of ZAP-70 (van Oers et al., 1996; Zamoyska et al., 2003; Palacios and Weiss, 2004). However, their role in receptor-proximal signaling by the BCR and Fc receptors is rather controversial. Although the combined deficiency of Lyn, Fyn, and Blk results in defective BCR-induced NF-κB activation, receptor-proximal BCR signaling (ITAM phosphorylation) is not affected (Saijo et al., 2003). Genetic deficiency of Lyn, the predominant Src family kinase in B cells, even leads to enhanced BCR signaling and B cell–mediated autoimmunity (Hibbs et al., 1995; Nishizumi et al., 1995; Chan et al., 1997). Similarly, both positive (Hibbs et al., 1995; Nishizumi and Yamamoto, 1997; Parravicini et al., 2002; Gomez et al., 2005; Falanga et al., 2012) and negative (Kawakami et al., 2000; Hernandez-Hansen et al., 2004; Odom et al., 2004; Gomez et al., 2005; Falanga et al., 2012) functions for Fyn and Lyn during Fc receptor signaling in mast cells have been reported. In addition, Hck$^{-/-}$Fgr$^{-/-}$ neutrophils respond normally to IgG immune complex–induced activation (Lowell et al., 1996) and Fc receptor–mediated phagocytosis of IgG-coated red blood cells is delayed but not blocked in Hck$^{-/-}$Fgr$^{-/-}$Lyn$^{-/-}$ macrophages (Fitzer-Attas et al., 2000; Lowell, 2004). The differential requirement for Src family kinases in TCR, BCR, and Fc receptor signaling is thought to derive from the fact that Syk, but not ZAP-70, is itself able to phosphorylate ITAM tyrosines (Rolli et al., 2002), making Src family kinases indispensable for signaling by the ZAP-70–coupled TCR but not by the Syk-coupled BCR and Fc receptors.

Autoantibody production and immune complex formation is one of the major mechanisms of autoimmunity-induced tissue damage. In vivo models of those processes include the K/B×N serum transfer arthritis (Korganow et al., 1999) and autoantibody-induced blistering skin diseases (Liu et al., 1993; Sitaru et al., 2002, 2005), which mimic important aspects of human rheumatoid arthritis, bullous pemphigoid, and epidermolysis bullosa acquisita. Activation of neutrophils or macrophages (Liu et al., 2000; Wipke and Allen, 2001; Sitaru et al., 2002, 2005; Solomon et al., 2005), recognition of immune complexes by Fcγ receptors (Ji et al., 2002; Sitaru et al., 2002, 2005), and β_2 integrin–mediated leukocyte recruitment (Watts et al., 2005; Liu et al., 2006; Chiriac et al., 2007; Monach et al., 2010; Németh et al., 2010) are indispensable for the development of those in vivo animal models.

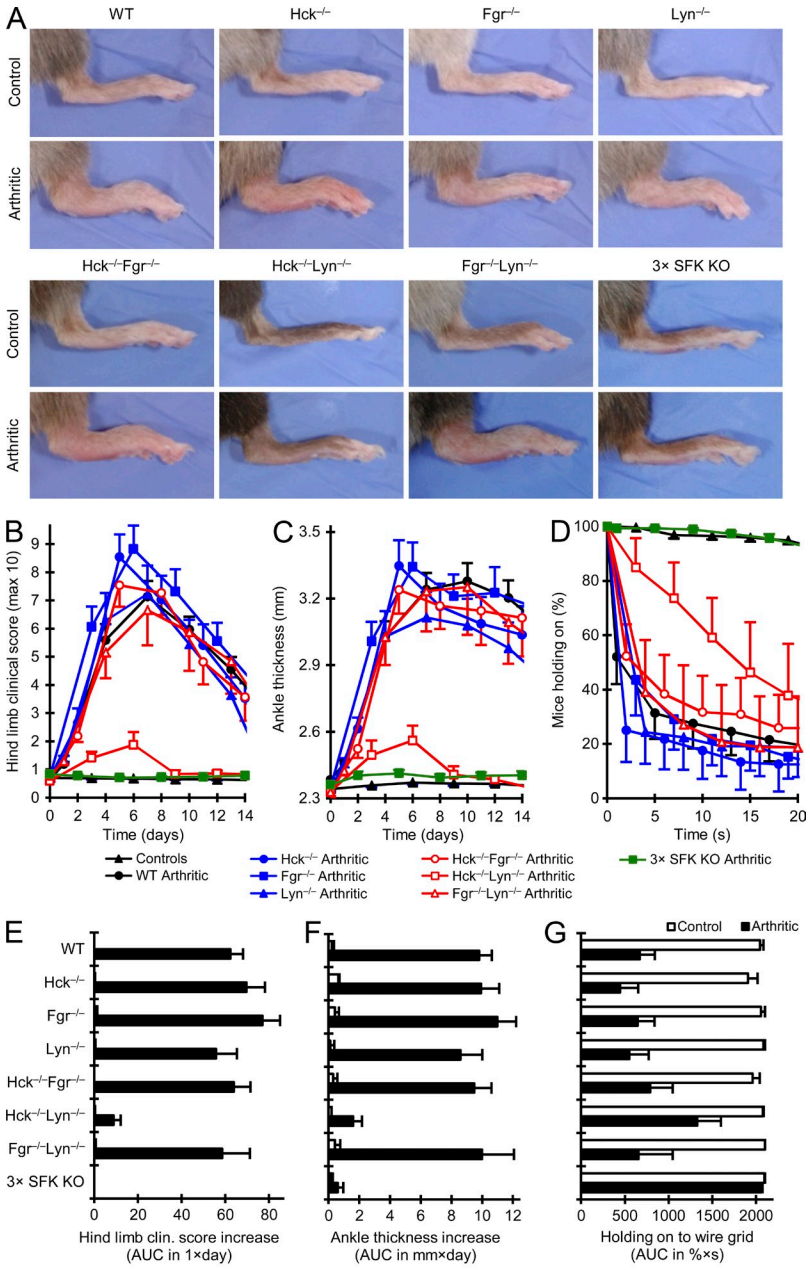

Figure 2. Overlapping role of Hck, Fgr, and Lyn during autoantibody-induced arthritis. (A) Arthritis was induced and assessed in WT, $Hck^{-/-}$, $Fgr^{-/-}$, and $Lyn^{-/-}$ single, $Hck^{-/-}Fgr^{-/-}$, $Hck^{-/-}Lyn^{-/-}$, and $Fgr^{-/-}Lyn^{-/-}$ double, and $Hck^{-/-}Fgr^{-/-}Lyn^{-/-}$ (3× SFK KO) triple knockout bone marrow chimeric mice as described in the Fig. 1 legend. Controls for all genotypes were combined in B–D. E–G show cumulative data obtained from the experiments shown in B–D. Images are representative of, and quantitative data show mean and SEM from 1–12 control and 7–26 arthritic serum-treated mice per genotype from 10 independent experiments. The joint functional test (D and G) were performed 3–24 times on each mouse between days 6 and 12. The WT and $Hck^{-/-}Fgr^{-/-}Lyn^{-/-}$ chimeric data include results presented in Fig. 1 (E–H). AUC, area under the curve.

The role of Src family kinases in β_2 integrin signaling and the requirement for β_2 integrins during autoantibody-induced in vivo inflammation prompted us to test the role of Src family kinases in autoantibody-induced inflammatory disease models. We found that $Hck^{-/-}Fgr^{-/-}Lyn^{-/-}$ mice were completely protected from autoantibody-induced arthritis and inflammatory blistering skin disease. Surprisingly, this was not due to a cell-autonomous defect in β_2 integrin–mediated leukocyte migration but to defective generation of an inflammatory microenvironment, likely due to the role of Src family kinases in immune complex–induced neutrophil and macrophage activation.

RESULTS

Hck, Fgr, and/or Lyn are required for autoantibody-induced arthritis

To determine the role of Src family kinases in autoantibody-induced arthritis, we first tested the development of K/B×N serum transfer arthritis in $Hck^{-/-}Fgr^{-/-}Lyn^{-/-}$ triple knockout mice. As shown in Fig. 1 A, administration of arthritogenic (K/B×N) serum triggered robust arthritis in WT but not $Hck^{-/-}Fgr^{-/-}Lyn^{-/-}$ animals. The $Hck^{-/-}Fgr^{-/-}Lyn^{-/-}$ mutation completely protected mice from disease development both in terms of visible clinical signs (Fig. 1 B; $P = 4.2 \times 10^{-5}$; $n = 6$) and ankle thickening (Fig. 1 C; $P = 4.5 \times 10^{-4}$;

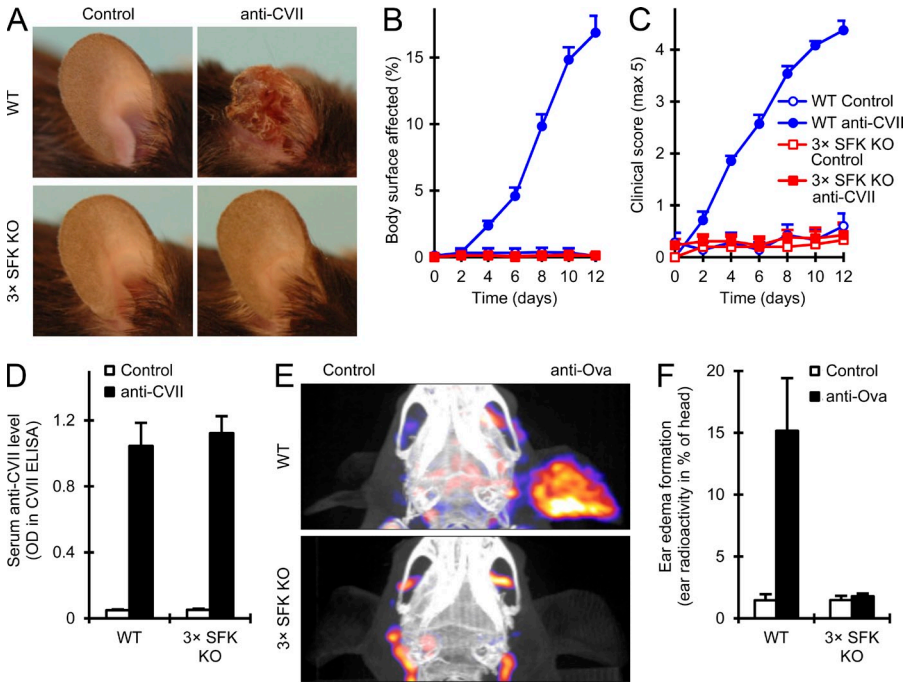

Figure 3. Src family kinases in autoantibody-induced skin blistering disease and the reverse passive Arthus reaction. (A–D) Blistering skin disease was triggered in WT or $Hck^{-/-}Fgr^{-/-}Lyn^{-/-}$ (3× SFK KO) mice or bone marrow chimeras by systemic injection of collagen VII–specific (α-CVII) antibodies. Skin disease was followed by photographing on day 14 (A) and clinical assessment of the total body surface affected (B) and the overall disease severity (C). The serum titer of α-CVII antibodies was tested on day 6 by ELISA (D). Representative images (A) or mean and SEM (B–D) from 5–7 control (1 intact and 4–6 bone marrow chimeric) and 13–14 α-CVII–treated (4 intact and 9–10 bone marrow chimeric) mice per genotype from 4 independent experiments are shown. No difference between intact and chimeric mice of the same hematopoietic genotype was observed (not depicted). (E and F) Reverse passive Arthus reaction was triggered in intact WT or $Hck^{-/-}Fgr^{-/-}Lyn^{-/-}$ (3× SFK KO) mice by systemic administration of ovalbumin, followed by intradermal injection of normal (control) or anti-ovalbumin (anti-Ova) rabbit serum into the left and right ears, respectively. Edema formation was assessed by determining the accumulation of radioactively labeled albumin from the circulation by NanoSPECT with a reference CT scan. Representative images (E) and mean and SEM (F) from 4–8 mice per genotype from 3 independent experiments are shown.

$n = 6$). We also tested the ability of the mice to hold onto the lower side of a wire grid as a measure of joint function (Jakus et al., 2009). Although the majority of arthritic serum-treated WT mice fell off the grid within a few seconds, most of the $Hck^{-/-}Fgr^{-/-}Lyn^{-/-}$ were able to hold onto the grid throughout the entire 20-second assay period (Fig. 1 D; $P = 9.5 \times 10^{-6}$; $n = 6$).

We also performed arthritis experiments in bone marrow chimeras generated by transplanting $Hck^{-/-}Fgr^{-/-}Lyn^{-/-}$ bone marrow cells to WT recipients or vice versa. As shown in Fig. 1 (E–H), bone marrow chimeras carrying $Hck^{-/-}Fgr^{-/-}Lyn^{-/-}$ bone marrow cells in a WT recipient were completely protected from all signs of K/B×N serum transfer arthritis ($P = 2.0 \times 10^{-12}$, 3.5×10^{-11}, and 1.2×10^{-7} for clinical score, ankle thickness, and joint functional assay, respectively; $n = 14–21$), whereas $Hck^{-/-}Fgr^{-/-}Lyn^{-/-}$ mice transplanted with WT bone marrow cells showed a normal disease course and an even somewhat more severe functional defect ($P = 0.36$, 0.59, and 0.028, respectively; $n = 7$). The above results indicate that expression of Hck, Fgr, and/or Lyn in the hematopoietic compartment is indispensable for the development of autoantibody-induced arthritis in experimental mice.

Overlapping role of Hck, Fgr, and Lyn during autoantibody-induced arthritis

We next tested K/B×N serum transfer arthritis in bone marrow chimeras with single or double deficiency of Hck, Fgr, or Lyn in the hematopoietic compartment. Representative hind limb images are shown in Fig. 2 A, quantitative analyses of arthritic serum-treated mice in Fig. 2 (B–D), and cumulated data for both control and arthritic serum-treated mice in Fig. 2 (E–G). Hck, Fgr, or Lyn single deficiency did not affect arthritis development in our model (p-values for clinical score, ankle thickness, and joint functional test were between 0.34 and 0.98; $n = 10–11$). $Hck^{-/-}Fgr^{-/-}$ and $Fgr^{-/-}Lyn^{-/-}$ double knockout chimeras showed no protection either ($0.086 \le P \le 0.99$; $n = 4–10$). The $Hck^{-/-}Lyn^{-/-}$ double mutation caused substantial but incomplete reduction of arthritis development ($P = 1.2 \times 10^{-10}$, 1.4×10^{-9}, and 0.031 for clinical score, ankle thickness, and joint functional test, respectively; $n = 5–7$); however, the poor overall health status of these chimeras (Xiao et al., 2008) may have affected their response in our model. Importantly, complete protection from arthritis development was only seen in the absence of all three kinases ($P = 2.0 \times 10^{-12}$, 3.5×10^{-11}, and 1.2×10^{-7}, respectively; $n = 14–21$), indicating significant functional overlap between Hck, Fgr, and Lyn during autoantibody-induced inflammation.

Other immune complex–induced inflammation models

We also tested the effect of the $Hck^{-/-}Fgr^{-/-}Lyn^{-/-}$ mutation on other autoantibody-induced inflammatory processes. Systemic administration of collagen VII–specific antibodies (a mouse model of the human blistering skin disease epidermolysis bullosa acquisita; Sitaru et al., 2005, 2007) triggered skin inflammation in WT but not $Hck^{-/-}Fgr^{-/-}Lyn^{-/-}$ mutant animals (Fig. 3 A). $Hck^{-/-}Fgr^{-/-}Lyn^{-/-}$ mutants were completely protected both in terms of the body surface area affected (Fig. 3 B; $P = 1.5 \times 10^{-10}$; $n = 11$) and the overall disease severity (Fig. 3 C; $P = 1.1 \times 10^{-10}$; $n = 13$). However, circulating collagen VII–specific antibody titers were not affected by the $Hck^{-/-}Fgr^{-/-}Lyn^{-/-}$

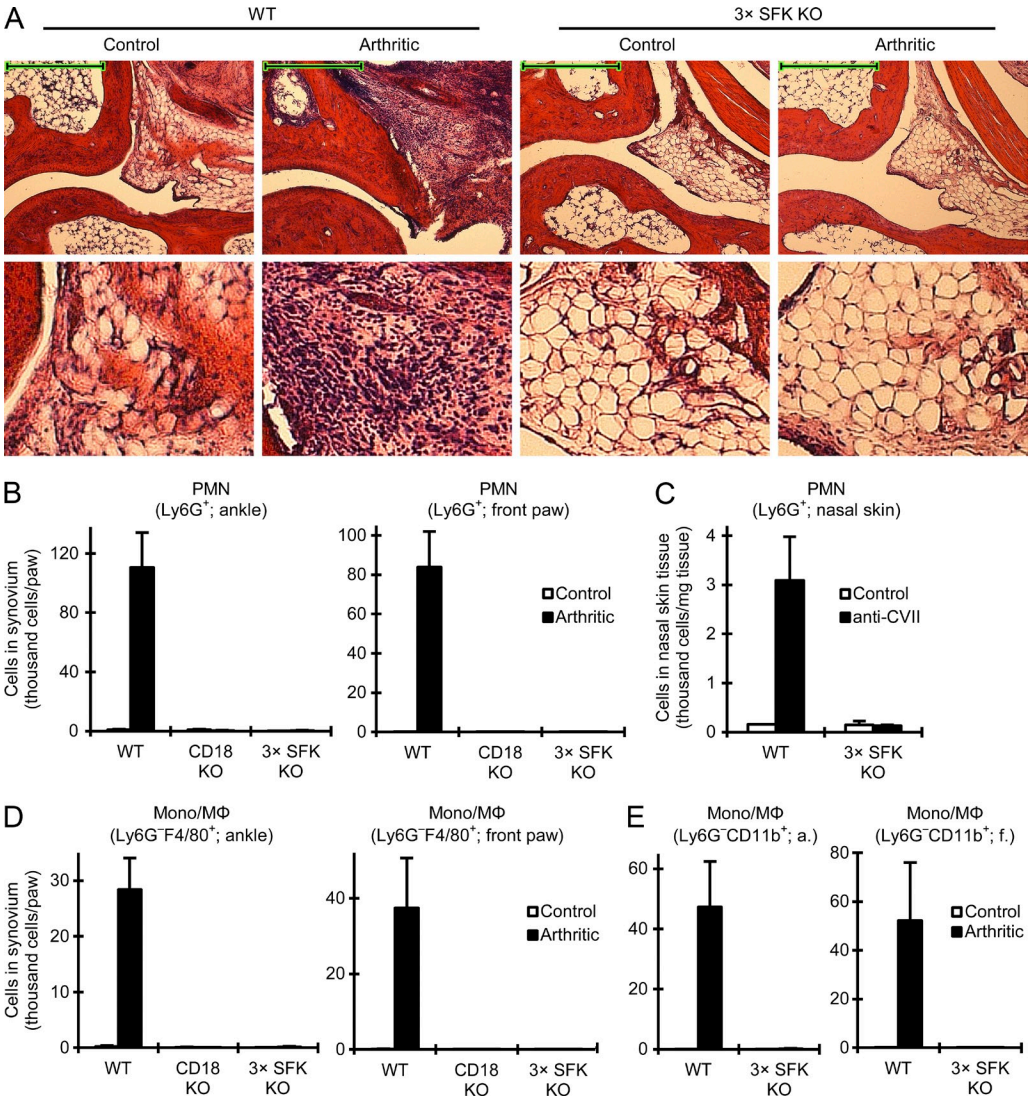

Figure 4. Myeloid cells fail to accumulate at the site of inflammation. Intact WT, CD18$^{-/-}$ (CD18 KO), or Hck$^{-/-}$Fgr$^{-/-}$Lyn$^{-/-}$ (3× SFK KO) mice were subjected to K/B×N serum transfer arthritis (A, B, D, and E) or autoantibody-induced skin blistering disease (C) as described in the legends to Figs. 1 and 3. (A) Hematoxylin-eosin–stained sections of ankle joints 7 d after the serum transfer. Images are representative of 4 control and 6 arthritic serum-treated mice per genotype from 2 independent experiments. Lower images were magnified from the upper sections. Bars, 200 µm. (B–D) The ankle area or the front paw was flushed (B, D, and E) or the nasal skin was digested (C), and the number of neutrophils (PMN; B and C) or monocytes/macrophages (mono/MΦ; D and E) was determined by flow cytometry. Graphs represent mean and SEM of data obtained from 3–7 control and 5–13 arthritic serum-treated mice per genotype from 2–5 independent experiments (B and D), 3–4 control and 6 arthritic serum-treated mice per genotype from 2 independent experiments (E), or 2 control and 4 anti-CVII–treated mice per genotype from 2 independent experiments (C). a., ankle; f., front paw.

mutation (Fig. 3 D; P = 0.34; n = 2). Importantly, intact Hck$^{-/-}$Fgr$^{-/-}$Lyn$^{-/-}$ mice and Hck$^{-/-}$Fgr$^{-/-}$Lyn$^{-/-}$ bone marrow chimeras were both completely protected from skin disease in our model (unpublished data).

We also tested the reverse passive Arthus reaction triggered by systemic administration of ovalbumin followed by intradermal injection of anti-ovalbumin into the ear. Edema formation was followed by imaging the accumulation of radioactively labeled albumin from the circulation. As shown in Fig. 3 (E and F), anti-ovalbumin injection caused robust increase of vascular permeability in WT but not Hck$^{-/-}$Fgr$^{-/-}$Lyn$^{-/-}$ animals (P = 0.013; n = 8). Collectively, Hck, Fgr, and Lyn are required for antibody-induced tissue damage in various in vivo inflammation models.

Myeloid cells fail to accumulate at the site of inflammation

We and others reported complete protection of CD18$^{-/-}$ mice from K/B×N serum transfer arthritis, likely due to a cell-autonomous role for LFA-1 in migration of myeloid cells to the site of inflammation (Watts et al., 2005; Németh et al., 2010; Monach et al., 2010). Given the role for Src family kinases in integrin signaling in myeloid cells and in autoantibody-induced

in vivo inflammation (Figs. 1–3), we next tested their role in leukocyte accumulation at the inflammatory site. As shown in Fig. 4 A, K/B×N serum transfer arthritis triggered robust leukocytic infiltration of the synovial area of WT but not $Hck^{-/-}Fgr^{-/-}Lyn^{-/-}$ mice. Flow cytometric analysis revealed a dramatic increase of neutrophil numbers in the synovial tissue of arthritic serum-treated WT mice that was entirely dependent on CD18 (Fig. 4 B; $P = 6.8 \times 10^{-5}$ and 1.6×10^{-4} for ankle and front limb, respectively; $n = 5$). Importantly, the $Hck^{-/-}Fgr^{-/-}Lyn^{-/-}$ mutation also abrogated neutrophil infiltration at the synovial area (Fig. 4 B; $P = 7.2 \times 10^{-5}$ and 1.7×10^{-4}, respectively; $n = 13$). The defective neutrophil infiltration was not due to reduced circulating numbers of neutrophils because blood neutrophil counts were even higher in both $CD18^{-/-}$ (10.7 ± 2.1 and 16.9 ± 5.7 thousand cells/μl before and on day 4 after K/B×N serum transfer, respectively; $n = 4$) and $Hck^{-/-}Fgr^{-/-}Lyn^{-/-}$ (2.5 ± 0.6 and 4.6 ± 1.6 thousand cells/μl, respectively; $n = 4$) than in WT animals (0.6 ± 0.1 and 1.4 ± 0.3 thousand cells/μl, respectively; $n = 4$).

We also tested neutrophil infiltration in the nasal skin during autoantibody-induced skin blistering disease. As shown in Fig. 4 C, neutrophils infiltrated the skin of WT but not $Hck^{-/-}Fgr^{-/-}Lyn^{-/-}$ animals ($P = 0.0088$; $n = 4$).

We next tested the accumulation of monocytes/macrophages. $Ly6G^{-}F4/80^{+}$ cells infiltrated the synovial area of arthritic serum-treated WT mice, and this was again entirely dependent on the presence of CD18 (Fig. 4 D; $P = 1.1 \times 10^{-4}$ and 1.6×10^{-4} for ankle and front paw, respectively; $n = 5$). The $Hck^{-/-}Fgr^{-/-}Lyn^{-/-}$ mutation also completely abrogated the accumulation of $Ly6G^{-}F4/80^{+}$ cells (Fig. 4 D; $P = 1.1 \times 10^{-4}$ and 1.7×10^{-4}, respectively; $n = 13$). Again, the defective infiltration was not due to reduced number of circulating monocytes because $Ly6G^{-}F4/80^{+}$ blood monocyte counts in $CD18^{-/-}$ (710 ± 144 and $1{,}591 \pm 351$ cells/μl on days 0 and 4, respectively; $n = 4$) and $Hck^{-/-}Fgr^{-/-}Lyn^{-/-}$ mice (553 ± 154 and 244 ± 59 cells/μl, respectively; $n = 4$) was similar to or higher than those in WT animals (433 ± 90 and 258 ± 40 cells/μl, respectively; $n = 4$). No infiltration of monocytes/macrophages identified as $Ly6G^{-}CD11b^{+}$ cells could be observed in the synovial area of $Hck^{-/-}Fgr^{-/-}Lyn^{-/-}$ mice either (Fig. 4 E; $P = 0.015$ and 0.031 for ankle and front paw, respectively; $n = 6$; this could not be tested in $CD18^{-/-}$ mice because their leukocytes do not express CD11b). Collectively, similar to the CD18 deficiency, the $Hck^{-/-}Fgr^{-/-}Lyn^{-/-}$ mutation also abrogates the accumulation of myeloid cells at the site of inflammation.

No cell-autonomous migration defect in $Hck^{-/-}Fgr^{-/-}Lyn^{-/-}$ myeloid cells

To reveal whether the defective leukocyte recruitment in $Hck^{-/-}Fgr^{-/-}Lyn^{-/-}$ mice is due to a cell-autonomous migration defect, we directly compared the accumulation of WT and mutant cells within the same animal. To this end, we generated mixed bone marrow chimeras carrying varying ratios of CD45.1-expressing WT, along with CD45.2-positive WT, $CD18^{-/-}$, or $Hck^{-/-}Fgr^{-/-}Lyn^{-/-}$ hematopoietic cells within the same animal (WT:WT, WT:$CD18^{-/-}$, and WT:$Hck^{-/-}Fgr^{-/-}Lyn^{-/-}$ chimeras, respectively). We then compared the percentage of CD45.2-positive cells in the blood and synovial tissue within the same individual mouse during K/B×N serum transfer arthritis.

In chimeras having CD45.2-expressing WT and CD45.1-expressing WT hematopoietic tissues (WT:WT chimeras), the percentage of CD45.2-positive neutrophils was similar in the blood and synovial infiltrate in all chimeras tested (Fig. 5 A). In contrast, in WT:$CD18^{-/-}$ chimeras (Fig. 5 B), the percentage of CD45.2-expressing (i.e., $CD18^{-/-}$) neutrophils in the inflamed synovium was much lower than that in the circulation, indicating a cell-autonomous recruitment defect of $CD18^{-/-}$ neutrophils. Surprisingly, in WT:$Hck^{-/-}Fgr^{-/-}Lyn^{-/-}$ chimeras (Fig. 5 C), no difference between the percentage of CD45.2-positive (i.e., $Hck^{-/-}Fgr^{-/-}Lyn^{-/-}$) neutrophils in the blood and the synovial infiltrate could be observed, indicating that $Hck^{-/-}Fgr^{-/-}Lyn^{-/-}$ neutrophils can accumulate normally at the site of inflammation when WT cells are also present in the same animal. The results of such experiments performed on a large cohort of mice are summarized in Fig. 5 D, where each dot represents an individual mouse. Although dots of WT:WT and WT:$Hck^{-/-}Fgr^{-/-}Lyn^{-/-}$ chimeras line up along the dotted line representing equal ratios in the blood and the synovium, dots of WT:$CD18^{-/-}$ chimeras are shifted to the lower right, indicating reduced ability of $CD18^{-/-}$ cells to enter the synovium from the circulation. The same data have also been used to calculate the relative migratory capacity of neutrophils of the different genotypes (Fig. 5 F). Those calculations confirmed a strong cell-autonomous recruitment defect of $CD18^{-/-}$ neutrophils ($P = 2.0 \times 10^{-12}$ and 1.0×10^{-9} for ankle and front paw, respectively; $n = 10$–14), whereas the accumulation of $Hck^{-/-}Fgr^{-/-}Lyn^{-/-}$ neutrophils was even slightly higher ($P = 0.021$ and 0.11, respectively; $n = 7$–15) than that of WT cells within the same animal.

We have also tested the accumulation of monocytes/macrophages in a similar manner. As shown in Fig. 5 (E and G), although CD18 deficiency caused a significant cell-autonomous reduction of the percentage of $Ly6G^{-}F4/80^{+}$ macrophages in the synovial tissue (relative to the percentage of $CD18^{-/-}$ cells among circulating $Ly6G^{-}F4/80^{+}$ monocytes; $P = 8.0 \times 10^{-6}$; $n = 7$), the $Hck^{-/-}Fgr^{-/-}Lyn^{-/-}$ mutation did not affect the accumulation of F4/80-positive cells in the inflamed synovium ($P = 0.83$; $n = 5$). The $Hck^{-/-}Fgr^{-/-}Lyn^{-/-}$ mutation had no effect on macrophage accumulation when the cells were identified as $Ly6G^{-}CD11b^{+}$ cells either (Fig. 5, E and G; $P = 0.37$; $n = 6$). Collectively, when WT cells are present in mixed bone marrow chimeras, $Hck^{-/-}Fgr^{-/-}Lyn^{-/-}$ neutrophils and monocytes/macrophages accumulate normally at the site of inflammation, arguing against a cell-autonomous migration defect of $Hck^{-/-}Fgr^{-/-}Lyn^{-/-}$ myeloid cells.

Normal in vitro migration of $Hck^{-/-}Fgr^{-/-}Lyn^{-/-}$ neutrophils and monocytes

We next tested the migration of neutrophils and monocytes in an in vitro Transwell assay. As shown in Fig. 5 H,

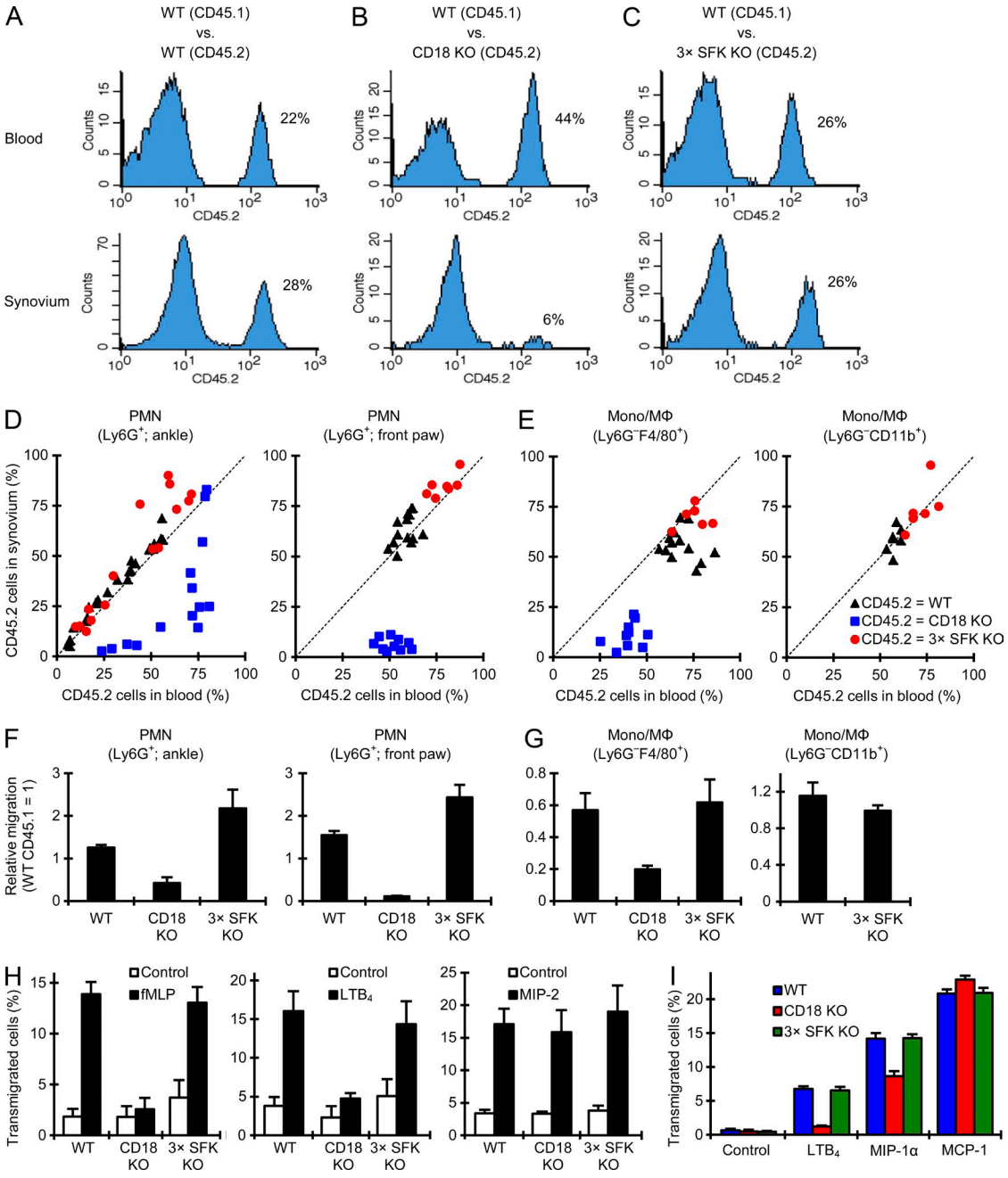

Figure 5. Normal in vitro and in vivo migration of Hck$^{-/-}$Fgr$^{-/-}$Lyn$^{-/-}$ neutrophils. (A–G) Mixed bone marrow chimeras with CD45.1-expressing WT and CD45.2-expressing WT, CD18$^{-/-}$ (CD18 KO), or Hck$^{-/-}$Fgr$^{-/-}$Lyn$^{-/-}$ (3× SFK KO) hematopoietic cells were subjected to K/B×N serum transfer arthritis as described in the Fig. 1 legend. In vivo accumulation of neutrophils (PMN; A–D and F) and monocytes/macrophages (Mono/MΦ; E and G) was determined by flushing the synovial area of arthritic serum-treated mixed bone marrow chimeras on day 4, followed by flow cytometric analysis of the ratio of CD45.1- and CD45.2-expressing cells in peripheral blood and the synovial infiltrate. A–C shows representative histograms of CD45.2 expression in blood or synovial neutrophils. In D and E, each dot represents an individual mouse. Bar graphs in F and G show mean and SEM of relative migration. Data are representative of (A–C) or summarize (D and F) data obtained from 7–26 mice per group from 3–9 independent experiments or 7–14 mice per group from 3–5 independent experiments (E and G). (H and I) In vitro migration of CD18$^{-/-}$ and Hck$^{-/-}$Fgr$^{-/-}$Lyn$^{-/-}$ bone marrow neutrophils (H) and monocytes (I) toward the indicated chemoattractants in a fibrinogen-coated Transwell system. Data represent mean and SEM of 3–13 (H) or 3–5 (I) independent experiments.

neutrophil migration toward fMLP (which mimics bacterial/mitochondrial-derived signals) was strongly reduced in CD18$^{-/-}$ ($P = 4.1 \times 10^{-4}$; $n = 4$) but not in Hck$^{-/-}$Fgr$^{-/-}$Lyn$^{-/-}$ cells ($P = 0.17$; $n = 4$). Similarly, neutrophil migration toward the lipid chemoattractant LTB_4 was dependent on CD18 ($P = 1.7 \times 10^{-6}$; $n = 3$) but was not affected by the Hck$^{-/-}$Fgr$^{-/-}$Lyn$^{-/-}$

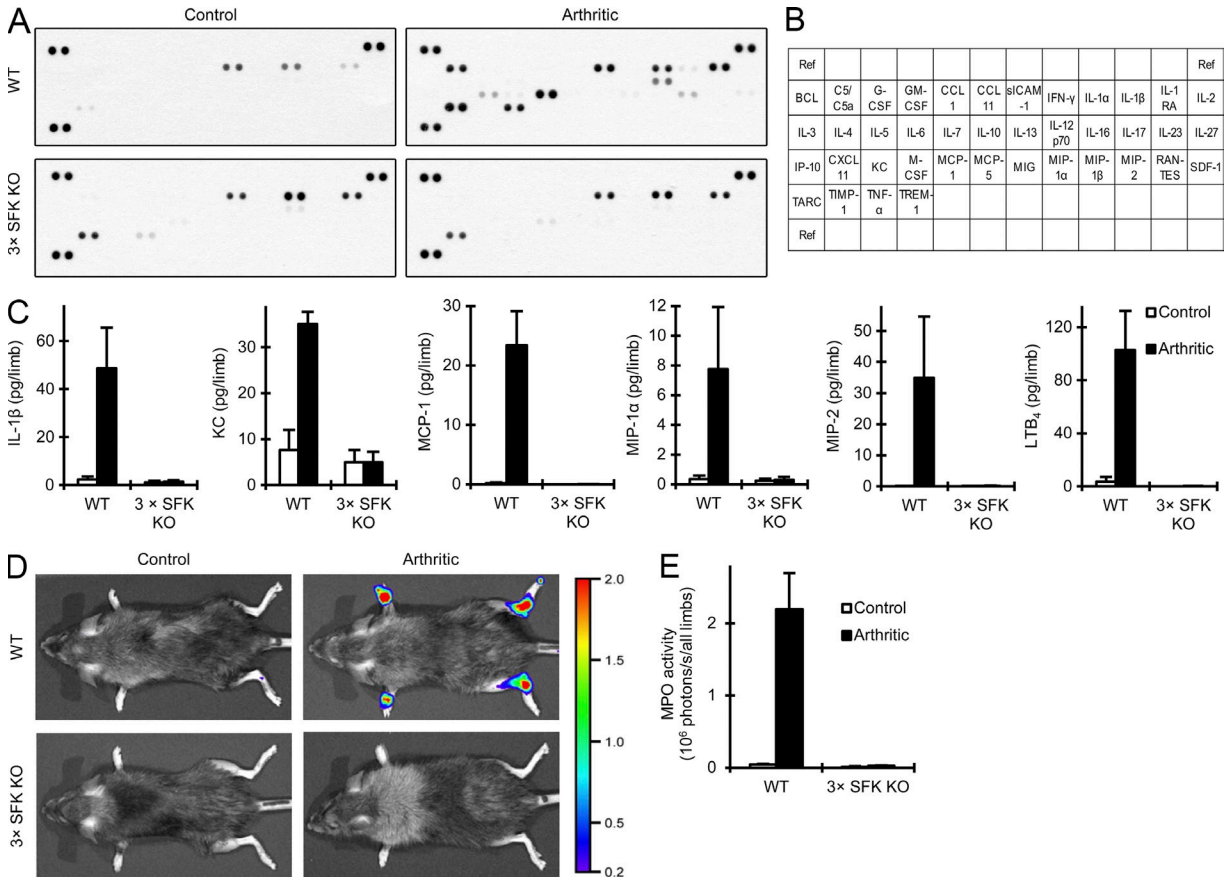

Figure 6. Myeloid Src family kinases are required for the generation of an inflammatory environment in vivo. Intact WT or Hck$^{-/-}$Fgr$^{-/-}$Lyn$^{-/-}$ (3× SFK KO) mice were subjected to K/B×N serum transfer arthritis as described in the legend to Fig. 1. (A and C) The synovial area was flushed on Day 4. The cell-free supernatants of the synovial infiltrates were probed using a commercial cytokine array (A) or by ELISA assays for the indicated pro-inflammatory mediators (C). (B) Map of the position of the different analytes on the cytokine array. A shows representative images from 2 independent experiments, whereas C shows mean and SEM of 4–6 mice per group from 3–5 independent experiments. (D-E) MPO activity was determined in vivo by chemiluminescence imaging after i.p. injection of luminol. Color-coded photon flux intensity is superposed on the grayscale photo of the mouse (D) and quantitated in defined regions of interest (E). Representative images (D) and mean and SEM (E) from 4 control and 6 arthritic serum-treated mice per genotype from 2 independent experiments are shown.

mutation (P = 0.41; n = 4). Interestingly, migration of neutrophils toward macrophage inflammatory protein 2 (MIP-2; CXCL2), a distant homologue of human IL-8, was not affected by either the CD18$^{-/-}$ (P = 0.58; n = 9) or the Hck$^{-/-}$Fgr$^{-/-}$Lyn$^{-/-}$ (P = 0.39; n = 7) mutation.

We have also tested the in vitro migration of freshly isolated bone marrow monocytes (Fig. 5 I). Monocyte migration toward leukotriene B_4 (LTB_4) was abrogated by CD18 deficiency (P = 0.0038; n = 3) but not by the Hck$^{-/-}$Fgr$^{-/-}$Lyn$^{-/-}$ mutation (P = 0.93; n = 5). Migration of monocytes toward MIP-1α (CCL3), one of the major monocyte chemoattractants, was also moderately reduced by the CD18$^{-/-}$ mutation with a borderline statistical significance (P = 0.057; n = 3), but it was normal in Hck$^{-/-}$Fgr$^{-/-}$Lyn$^{-/-}$ cells (P = 0.63; n = 5). The migration of the cells toward monocyte chemoattractant protein 1 (MCP-1; CCL2), another major monocyte chemoattractant, was slightly even increased by CD18 deficiency (P = 0.0039; n = 3), but it was not affected by the Hck$^{-/-}$Fgr$^{-/-}$Lyn$^{-/-}$ mutation (P = 0.74; n = 5). Collectively, in vitro migration of neutrophils and monocytes toward major proinflammatory chemoattractants does not depend on Hck, Fgr, or Lyn irrespective of the requirement for β_2 integrins in the given assay.

Defective generation of the inflammatory environment

The above observations could be explained by a role for myeloid Src family kinases in the generation of the inflammatory environment. As shown in the cytokine arrays in Fig. 6 A (see array map in Fig. 6 B and quantification in Table S1), K/B×N serum transfer arthritis triggered robust accumulation of various inflammatory mediators in the synovial tissue of WT but not Hck$^{-/-}$Fgr$^{-/-}$Lyn$^{-/-}$ animals. Prior studies suggested important roles for IL-1β, keratinocyte chemoattractant (KC; CXCL1), MIP-1α, MIP-2, and LTB_4 in myeloid cell infiltration during autoantibody-induced inflammation (Kim et al., 2006; Chou et al., 2010; Jacobs et al., 2010), whereas MCP-1 is considered a major monocyte chemoattractant (Deshmane et al., 2009). ELISA assays (Fig. 6 C) confirmed

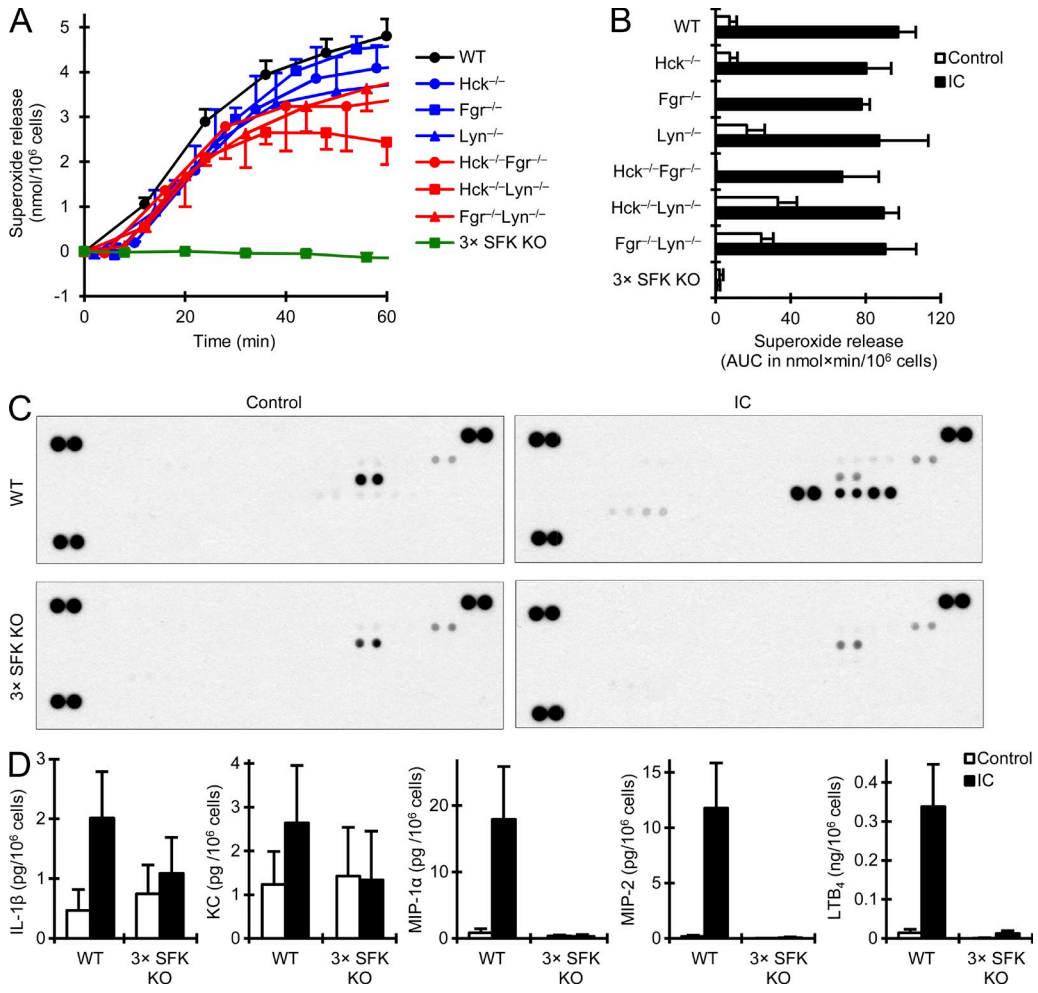

Figure 7. Hck$^{-/-}$Fgr$^{-/-}$Lyn$^{-/-}$ neutrophils fail to respond to immune complex stimulation. WT, Hck$^{-/-}$Fgr$^{-/-}$Lyn$^{-/-}$ (3× SFK KO), and the various single and double knockout neutrophils were placed on immobilized immune complex (IC) surfaces. Superoxide release (A and B) was followed by a spectrophotometric assay. Cytokine, chemokine, and lipid mediator levels in cell-free supernatants were determined after an incubation for 1 h (LTB_4) or 6 h (all other readouts) using a commercial cytokine array (C) or ELISA assays (D). Graphs in A and B show mean and SEM of 3–22 independent experiments per genotype. Values at the zero time point were subtracted. C is representative of 2 independent experiments. D shows mean and SEM from 4–11 independent experiments.

that the Hck$^{-/-}$Fgr$^{-/-}$Lyn$^{-/-}$ mutation abrogated the up-regulation of IL-1β ($P = 0.0026$; $n = 5$), KC ($P = 9.0 \times 10^{-7}$; $n = 5$), MCP-1 ($P = 0.0014$; $n = 5$), MIP-2 ($P = 0.023$; $n = 6$), and LTB_4 ($P = 7.4 \times 10^{-15}$; $n = 3$) in the synovial tissue and caused a substantial (though not statistically significant) reduction of MIP-1α levels ($P = 0.095$; $n = 4$).

We have also tested the generation of reactive oxygen species (ROS) and the release of granule enzymes into the extracellular space at the inflammatory site by in vivo imaging of the activity of myeloperoxidase (MPO), a neutrophil granule-derived ROS-producing enzyme (Gross et al., 2009; Nussbaum et al., 2013). As shown in Fig. 6 (D and E), K/B×N serum transfer arthritis triggered a robust ROS bioluminescence signal localized to the ankles and front paws in WT but not Hck$^{-/-}$Fgr$^{-/-}$Lyn$^{-/-}$ mutant animals ($P = 0.010$; $n = 6$). Collectively, myeloid Src family kinases are required for various aspects of the generation of a proinflammatory environment during autoantibody-induced arthritis.

Hck$^{-/-}$Fgr$^{-/-}$Lyn$^{-/-}$ myeloid cells fail to respond to immune complex stimulation

To test whether Src family kinases are directly involved in the generation of an inflammatory environment, we investigated immune complex–induced in vitro responses of neutrophils and macrophages. As shown in Fig. 7 (A and B), the Hck$^{-/-}$Fgr$^{-/-}$Lyn$^{-/-}$ mutation completely blocked immune complex–induced superoxide release from neutrophils ($P = 2.4 \times 10^{-21}$; $n = 15$). Similar to the in vivo findings with K/B×N serum transfer arthritis (Fig. 2), the Hck$^{-/-}$Lyn$^{-/-}$ mutation caused a partial but statistically significant reduction ($P = 5.8 \times 10^{-4}$; $n = 4$; this may in part be due to increased basal levels in those samples), whereas the other single or double knockouts had no significant defect (Fig. 7, A and B; $0.10 < P < 0.71$; $n = 3$).

As shown in the cytokine arrays in Fig. 7 C (see array map in Fig. 6 B and quantification in Table S1), immune complex stimulation also triggered the release of several cytokines and chemokines from WT but not Hck$^{-/-}$Fgr$^{-/-}$Lyn$^{-/-}$ neutrophils.

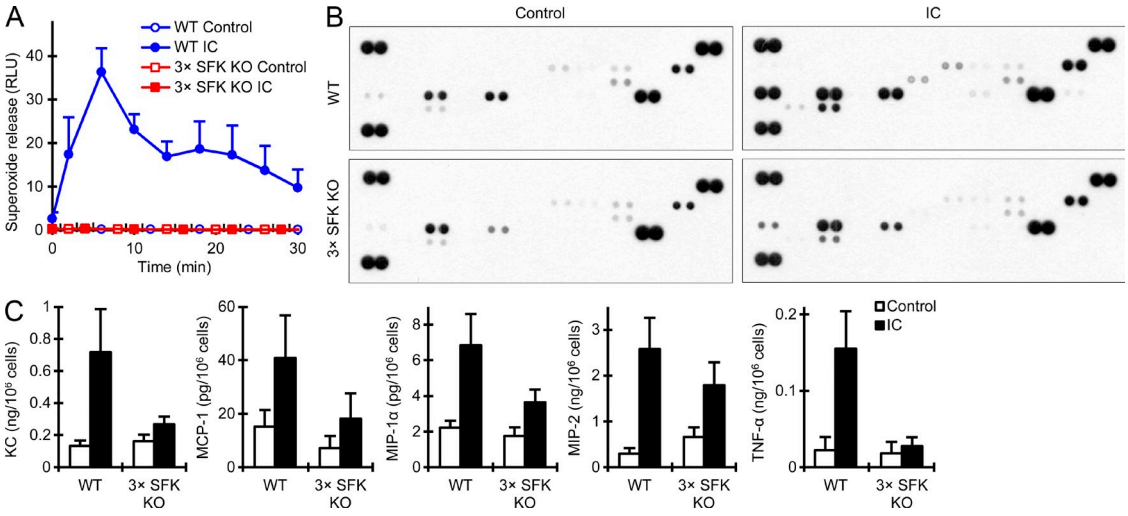

Figure 8. Defective responses of Hck$^{-/-}$Fgr$^{-/-}$Lyn$^{-/-}$ macrophages to immune complex stimulation. Bone marrow–derived WT or Hck$^{-/-}$Fgr$^{-/-}$Lyn$^{-/-}$ (3× SFK KO) macrophages were placed on immobilized immune complex (IC) surfaces. Their superoxide release (A) was followed by a luminometric assay. Cytokine and chemokine levels from the cell-free supernatants taken after 24 h were tested by a commercial cytokine array (B) or by ELISA assays (C). A shows mean and SEM from 4 independent experiments. B is representative of 2 experiments. C shows mean and SEM of data from 4–5 independent experiments.

ELISA assays revealed that the Hck$^{-/-}$Fgr$^{-/-}$Lyn$^{-/-}$ mutation dramatically reduced or even completely abrogated the immune complex–induced release of IL-1β ($P = 5.1 \times 10^{-5}$; $n = 6$), KC ($P = 3.6 \times 10^{-5}$; $n = 6$), MIP-1α ($P = 5.0 \times 10^{-6}$; $n = 6$), MIP-2 ($P = 4.8 \times 10^{-15}$; $n = 11$), and LTB_4 ($P = 8.8 \times 10^{-5}$; $n = 4$) from neutrophils (Fig. 7 D), whereas no release of MCP-1 could be observed even from WT cells (not depicted).

We also tested the immune complex–induced responses of bone marrow–derived macrophages. As shown in Fig. 8 A, the Hck$^{-/-}$Fgr$^{-/-}$Lyn$^{-/-}$ mutation completely blocked immune complex–induced ROS production by macrophages ($P = 2.8 \times 10^{-8}$; $n = 4$). The cytokine arrays shown in Fig. 8 B (see array map in Fig. 6 B and quantification in Table S1) indicated immune complex–induced release of various proinflammatory cytokines from WT macrophages which was strongly reduced in Hck$^{-/-}$Fgr$^{-/-}$Lyn$^{-/-}$ cultures. ELISA assays (Fig. 8 C) confirmed that the Hck$^{-/-}$Fgr$^{-/-}$Lyn$^{-/-}$ mutation strongly inhibited the immune complex–induced release of KC ($P = 0.0013$; $n = 5$), MCP-1 ($P = 0.010$; $n = 4$), and TNF ($P = 4.0 \times 10^{-4}$; $n = 4$) from macrophages, caused a partial but statistically significant inhibition of MIP-2 release ($P = 0.027$; $n = 4$), and led to an apparent reduction of MIP-1α release which, however, did not reach statistical significance ($P = 0.29$; $n = 4$). In contrast, no release of IL-1β or LTB_4 could be observed even in WT cultures (unpublished data). Collectively, the genetic deficiency of Hck, Fgr, and Lyn blocks the immune complex–induced release of various components of the inflammatory environment from both neutrophils and macrophages.

Src family kinases are required for initial Fc receptor signaling in neutrophils

Prior studies indicated that Src family kinases are critically involved in integrin- but not Fc receptor–mediated functional responses of myeloid cells (Lowell et al., 1996; Meng and Lowell, 1998; Mócsai et al., 1999; Suen et al., 1999; Fitzer-Attas et al., 2000; Pereira et al., 2001; Lowell, 2004). Our above observations led us to reevaluate this issue.

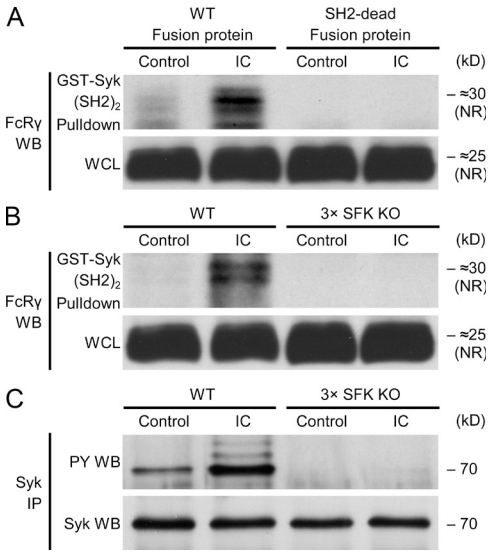

Figure 9. Src family kinases are required for immune complex–induced phosphorylation of FcRγ and Syk. (A–C) WT or Hck$^{-/-}$Fgr$^{-/-}$Lyn$^{-/-}$ (3× SFK KO) neutrophils were plated on immobilized IgG immune complexes (IC). Cell lysates were subjected to a GST pulldown assay (A and B) using either WT or R41A/R194A double mutant (SH2-Dead) GST-Syk(SH2)$_2$ fusion protein and probed for the presence of FcRγ by Western blotting (WB), or processed for Syk immunoprecipitation (IP), followed by immunoblotting for phosphotyrosine (PY) or Syk as a loading control (C). Whole cell lysates (WCL) served as loading control in A and B. Blots in A–C are representative of 3 independent experiments. Note substantial mobility shift caused by the tyrosine phosphorylation of FcRγ homodimers under the used nonreducing (NR) conditions in A and B. WB, Western blot.

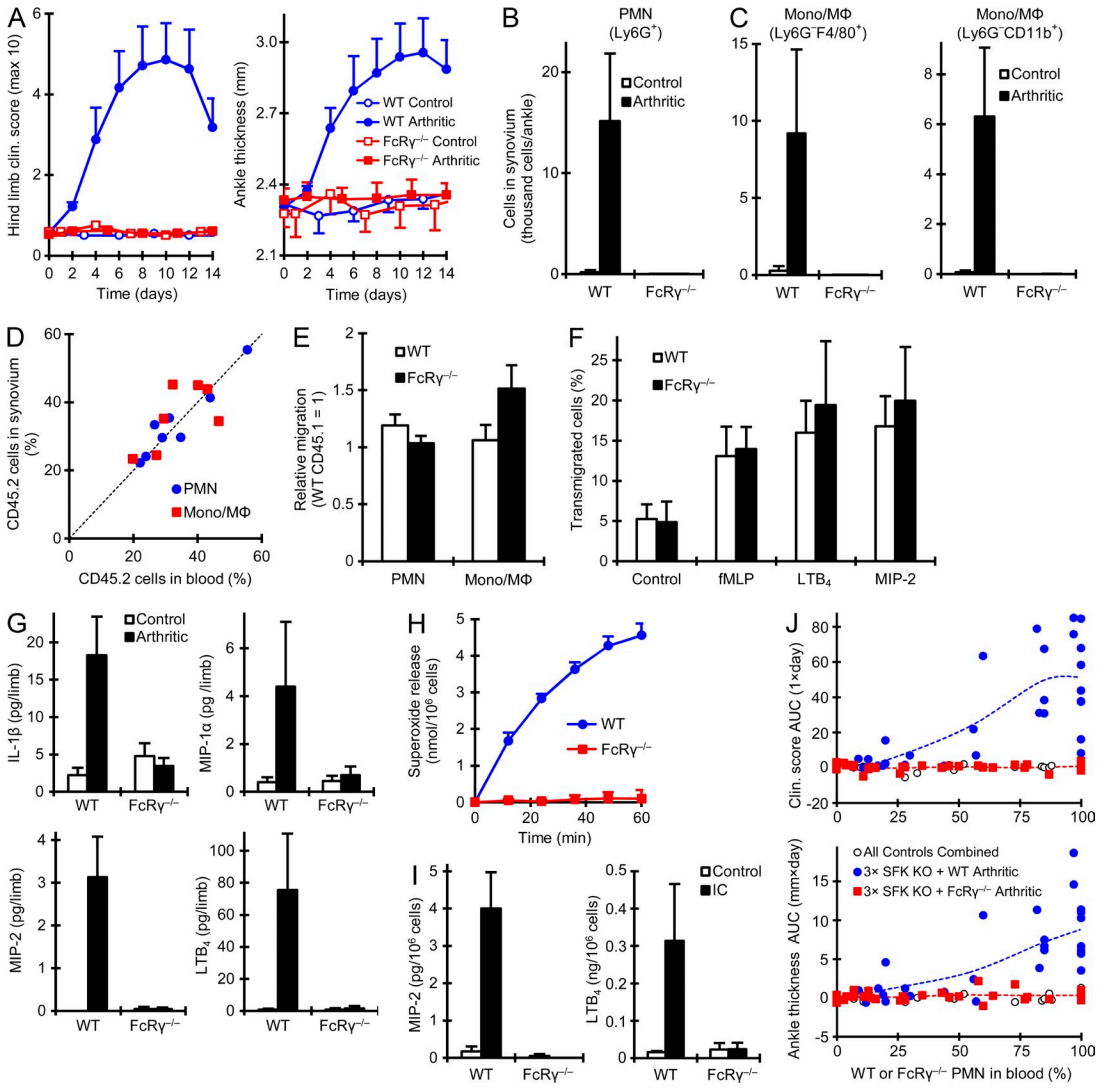

Figure 10. FcRγ deficiency phenocopies the deficiency of Src family kinases. (A–C) K/B×N serum transfer arthritis was induced in intact WT and FcRγ$^{-/-}$ mice as described in the Fig. 1 legend, followed by analysis of the clinical disease course as described in Fig. 1 A (3 control and 5–7 arthritic mice per genotype from 3 independent experiments) or the quantification of leukocyte infiltration as described in Fig. 4 (B and C; 2–3 control and 6 arthritic mice per genotype from 3 independent experiments). (D and E) In vivo migration of neutrophils (PMN) and monocytes/macrophages (Mono/MΦ) determined using mixed bone marrow chimeras containing CD45.1-expressing WT and CD45.2-expressing FcRγ$^{-/-}$ cells as described in Fig. 5. Each dot in D represents an individual mouse. E shows mean and SEM of relative migration. (D and E) Data were obtained from 6–8 mice per group from 3 independent experiments. (F) In vitro migration of WT and FcRγ$^{-/-}$ neutrophils tested as described in Fig. 5. Data were obtained from 3 independent experiments. (G) Inflammatory mediator release from WT and FcRγ$^{-/-}$ mice determined as described in Fig. 6. Data were obtained from 3–5 mice per group from 3 independent experiments. (H and I) Superoxide (H) or cytokine/chemokine/lipid mediator (I) release from immune complex-activated WT and FcRγ$^{-/-}$ neutrophils from intact mice was determined as described in Fig. 7. Data were obtained from 4 (H) or 3 (I) independent experiments. (J) Bone marrow chimeras generated by transplanting FcRγ$^{-/-}$ or CD45.1-expressing WT bone marrow cells mixed with Hck$^{-/-}$Fgr$^{-/-}$Lyn$^{-/-}$ cells at varying ratios were subjected to K/B×N serum transfer arthritis as described in Fig. 1. Area under the curve (AUC) values for daily clinical scoring and ankle thickness measurements are shown in relation to the percentage of WT or FcRγ$^{-/-}$ (i.e., non-Hck$^{-/-}$Fgr$^{-/-}$Lyn$^{-/-}$) cells in the peripheral blood. Data represent results from 8–13 control and 28–32 arthritic serum-treated mice per group from 3 independent experiments. All error bars show SEM from the indicated number of mice or experiments.

We first tested the phosphorylation of the Fc receptor γ-chain (FcRγ), the ITAM-containing signaling chain of activating Fc receptors. As shown in Fig. 9 A, a glutathione S-transferase (GST) fusion protein of the tandem SH2 domains of Syk (GST-Syk(SH2)$_2$) was able to pull down FcRγ from lysates of immune complex–activated WT neutrophils, whereas no such signal could be observed upon functional disruption of both SH2 domains (Mócsai et al., 2006), indicating that this assay specifically detects phosphorylation of the FcRγ ITAM tyrosines. Importantly, no FcRγ phosphorylation could be observed in lysates of immune complex–stimulated Hck$^{-/-}$Fgr$^{-/-}$Lyn$^{-/-}$ neutrophils (Fig. 9 B).

We next tested the activation of the Syk tyrosine kinase. As shown in Fig. 9 C, immune complex–induced neutrophil activation led to tyrosine phosphorylation of Syk in WT but not $Hck^{-/-}Fgr^{-/-}Lyn^{-/-}$ neutrophils. The above results indicate an indispensable role for Src family kinases in receptor-proximal Fc receptor signaling in neutrophils.

FcRγ deficiency recapitulates the phenotypes of $Hck^{-/-}Fgr^{-/-}Lyn^{-/-}$ mutants

The apparent role of Src family kinases in Fc receptor signaling prompted us to test the deficiency of $FcR\gamma^{-/-}$ mice (which lack all activating Fcγ receptors; Takai et al., 1994; Bruhns, 2012) in more detail. In agreement with previous studies (Ji et al., 2002; Corr and Crain, 2002), $FcR\gamma^{-/-}$ mice were completely protected from clinical signs of arthritis development in the K/B×N serum transfer model (Fig. 10 A; $P = 0.0033$ and 0.0039 for clinical score and ankle thickness, respectively; $n = 5$).

As shown in Fig. 10 (B and C), no accumulation of neutrophils ($P = 0.028$; $n = 6$) or of monocytes/macrophages defined either as $Ly6G^{-}F4/80^{+}$ ($P = 0.040$; $n = 6$) or $Ly6G^{-}CD11b^{+}$ ($P = 0.042$; $n = 6$) cells could be observed in the ankle synovium in $FcR\gamma^{-/-}$ mice. In contrast, in mixed bone marrow chimeras where WT hematopoietic cells were also present (Fig. 10, D and E), the $FcR\gamma^{-/-}$ mutation did not affect the accumulation of neutrophils ($P = 0.27$; $n = 8$) or macrophages ($P = 0.13$; $n = 8$) in the synovial tissue (normalized to the percentage of circulating $FcR\gamma^{-/-}$ neutrophils and monocytes, respectively). $FcR\gamma^{-/-}$ neutrophils also migrated normally toward fMLP, LTB_4, and MIP-2 in vitro (Fig. 10 F; $0.42 < P < 0.46$; $n = 3$).

We also tested typical components of the inflammatory environment. FcRγ deficiency prevented the increase of IL-1β ($P = 0.017$; $n = 5$), KC ($P = 0.026$; $n = 5$), MCP-1 ($P = 1.5 \times 10^{-5}$; $n = 4$), MIP-1α ($P = 0.023$; $n = 3$), MIP-2 ($P = 0.025$; $n = 4$), and LTB_4 ($P = 0.016$; $n = 5$) in the synovial tissue of K/B×N serum-treated mice (Fig. 10 G and not depicted). As reported before (Jakus et al., 2008), $FcR\gamma^{-/-}$ neutrophils failed to release superoxide when plated on an immobilized IgG immune complex surface in vitro (Fig. 10 H; $P = 7.4 \times 10^{-5}$; $n = 4$). FcRγ deficiency also completely blocked the immune complex–induced release of IL-1β ($P = 0.0020$; $n = 3$), KC ($P = 0.038$; $n = 3$), MIP-1α ($P = 0.031$; $n = 3$), MIP-2 ($P = 5.2 \times 10^{-4}$; $n = 3$), and LTB_4 ($P = 0.013$; $n = 3$) from neutrophils (Fig. 10 I and not depicted).

All the above experiments indicated that the $Hck^{-/-}Fgr^{-/-}Lyn^{-/-}$ and the $FcR\gamma^{-/-}$ mutations cause similar phenotypes in our in vitro and in vivo models of autoantibody-induced inflammatory reactions. To provide further evidence for the functional overlap between Src family kinases and FcRγ, we tested whether $FcR\gamma^{-/-}$ hematopoietic cells can rescue arthritis development in $Hck^{-/-}Fgr^{-/-}Lyn^{-/-}$ mutants. To this end, we generated mixed bone marrow chimeras carrying $Hck^{-/-}Fgr^{-/-}Lyn^{-/-}$ hematopoietic system mixed with WT or $FcR\gamma^{-/-}$ hematopoietic cells, and we tested arthritis development in those chimeras. As shown in Fig. 10 J, the presence of WT hematopoietic tissues in addition to $Hck^{-/-}Fgr^{-/-}Lyn^{-/-}$ restored arthritis development. Obvious arthritis was clearly seen at ∼50% WT neutrophils in the circulation and the severity of arthritis further increased with increasing percentage of WT cells. In contrast, mixing $Hck^{-/-}Fgr^{-/-}Lyn^{-/-}$ and $FcR\gamma^{-/-}$ hematopoietic tissues did not result in any signs of arthritis development in the resulting chimeras at any ratio of the two genotypes in the circulating neutrophil pool. Collectively, the in vivo and in vitro phenotypes of $Hck^{-/-}Fgr^{-/-}Lyn^{-/-}$ and $FcR\gamma^{-/-}$ mutants are strikingly similar and $FcR\gamma^{-/-}$ cells cannot restore arthritis development on the $Hck^{-/-}Fgr^{-/-}Lyn^{-/-}$ background, suggesting a functional overlap between Src family kinases and Fcγ receptors.

DISCUSSION

Our experiments have revealed complete protection of $Hck^{-/-}Fgr^{-/-}Lyn^{-/-}$ mice from K/B×N serum transfer arthritis, autoantibody-induced skin blistering, and the reverse passive Arthus reaction (Figs. 1 and 3). Hck, Fgr, and Lyn were required in the hematopoietic compartment (Fig. 1, E–H) and showed significant functional overlap with each other (Fig. 2).

The overall phenotype of $Hck^{-/-}Fgr^{-/-}Lyn^{-/-}$ mutants was very similar to that of β_2 integrin–deficient ($CD18^{-/-}$) mice (Watts et al., 2005; Liu et al., 2006; Chiriac et al., 2007; Németh et al., 2010). β_2 integrins have long been known to mediate leukocyte migration to the site of inflammation (Mizgerd et al., 1997; Scharffetter-Kochanek et al., 1998; Walzog et al., 1999; Schymeinsky et al., 2007). Indeed, we observed a complete defect of leukocyte infiltration into the synovial tissue of $CD18^{-/-}$ animals (Fig. 4), and our mixed bone marrow chimeric experiments (Fig. 5, A–G) indicated, in agreement with a prior report (Monach et al., 2010), that $CD18^{-/-}$ myeloid cells had a cell-autonomous leukocyte migration defect. The similarities of the $CD18^{-/-}$ and $Hck^{-/-}Fgr^{-/-}Lyn^{-/-}$ phenotypes and the defective leukocyte infiltration in $Hck^{-/-}Fgr^{-/-}Lyn^{-/-}$ mice (Fig. 4) suggested that $Hck^{-/-}Fgr^{-/-}Lyn^{-/-}$ leukocytes have an intrinsic migration defect. However, $Hck^{-/-}Fgr^{-/-}Lyn^{-/-}$ myeloid cells accumulated normally in the inflamed synovium in mixed bone marrow chimeras (Fig. 5, A–G) and showed no in vitro migration defects either (Fig. 5, H and I). In contrast, they failed to release inflammatory mediators when activated by immobilized immune complexes in vitro (Fig. 7 and 8). Therefore, the arthritis defect in $Hck^{-/-}Fgr^{-/-}Lyn^{-/-}$ mice is likely due to the defective generation of an inflammatory environment rather than, as initially expected, to a cell-autonomous defect of β_2 integrin–mediated leukocyte migration.

Our results, in agreement with prior studies (Kim et al., 2006; Chen et al., 2006; Chou et al., 2010), indicate the existence of positive-feedback loops acting through the release of proinflammatory mediators (including IL-1β, neutrophil and monocyte/macrophage chemokines, and LTB_4) from myeloid cells that attract further myeloid cells to the site of inflammation. β_2 integrins and Src family kinases apparently function at different points of the feedback loop; whereas the former are required for the intrinsic migratory ability of leukocytes, the latter are involved in the release of proinflammatory mediators.

Nevertheless, due to the nature of autoamplification loops, the CD18$^{-/-}$ and the Hck$^{-/-}$Fgr$^{-/-}$Lyn$^{-/-}$ mutations both abrogate the entire inflammation process.

Although several prior reports proposed important roles for Src family kinases in in vitro (Fumagalli et al., 2007; Sarantos et al., 2008) and in vivo (Lowell and Berton, 1998; Meng and Lowell, 1998; Vicentini et al., 2002) migration of myeloid cells, several other studies came to the opposite conclusion (Mócsai et al., 2002; Zhang et al., 2005; Hirahashi et al., 2006; Yoo et al., 2011). The interpretation of those studies is hindered by their limited scope (Lowell and Berton, 1998; Sarantos et al., 2008), apparently contradicting results (Meng and Lowell, 1998; Mócsai et al., 2002; Zhang et al., 2005), indications of indirect effects on leukocyte migration (Vicentini et al., 2002), or defects seen only in unique in vitro assay systems (Fumagalli et al., 2007; Sarantos et al., 2008). Though our studies confirm the overall requirement for Src family kinases in leukocyte migration to the site of inflammation (Fig. 4), we conclude that this is not due to an intrinsic migration defect but to defective generation of the inflammatory environment. We nevertheless believe that certain specific in vitro conditions (such as very narrow Transwell pore sizes, transmigration through tightly sealed endothelial monolayers, or truly two-dimensional assays) may favor leukocyte migration in a Src family–dependent manner. In this context, it is interesting to note that dasatinib, an inhibitor of Src family kinases, blocked human neutrophil migration in a two-dimensional Zigmond chamber assay but not in various three-dimensional assays (Futosi et al., 2012). Similarly, the Hck$^{-/-}$Fgr$^{-/-}$Lyn$^{-/-}$ mutation partially reduced (but did not abrogate) neutrophil migration toward fMLP in a two-dimensional Zigmond chamber assay but not within a three-dimensional collagen gel (Barbara Walzog, personal communication). Further internally controlled in vivo experiments and detailed imaging studies, as well as analysis of other (e. g. microbial) chemotactic agents, will be needed to reveal the full spectrum of the contribution (or the lack of contribution) of Src family kinases to in vitro and in vivo migration of myeloid cells.

Several studies indicated a critical role for Src family kinases in β_2 integrin–mediated neutrophil and macrophage activation (Lowell et al., 1996; Mócsai et al., 1999; Suen et al., 1999; Giagulli et al., 2006). In agreement with those studies, both CD18$^{-/-}$ and Hck$^{-/-}$Fgr$^{-/-}$Lyn$^{-/-}$ neutrophils failed to adhere to an ICAM1-coated surface (unpublished data). This is in sharp contrast to the normal β_2 integrin–mediated migration of Hck$^{-/-}$Fgr$^{-/-}$Lyn$^{-/-}$ neutrophils and macrophages (Fig. 5). Though those results suggest that Src family–mediated outside-in signaling of β_2 integrins and the resulting cellular responses (e.g., cell spreading) are not required for β_2 integrin–mediated leukocyte migration, additional studies will be needed to fully clarify that issue.

It should also be mentioned that a prior study revealed integrin-independent leukocyte migration in three-dimensional environments (Lämmermann et al., 2008). Though it would be tempting to speculate that the normal in vivo recruitment of Hck$^{-/-}$Fgr$^{-/-}$Lyn$^{-/-}$ myeloid cells in mixed bone marrow chimeras is due to such integrin-independent mechanisms, the clear cell-autonomous requirement for CD18 (Fig. 5, A–G) indicates that this is not the case. Eosinophils comprised 19 ± 4% of circulating granulocytes but only 1.1 ± 0.7% of granulocytes in the synovial infiltrate (n = 5 mice per group), and eosinophil-deficient mice were even hyperresponsive in K/B×N serum transfer arthritis (Chen et al., 2014). Despite some controversy (Lee et al., 2002; Zhou et al., 2007; Feyerabend et al., 2011), our current understanding is that mast cells and basophils do not make a substantial contribution to autoantibody-induced arthritis either. Those points argue against a major contribution of eosinophils and mast cells/basophils to autoantibody-induced inflammation and the Hck$^{-/-}$Fgr$^{-/-}$Lyn$^{-/-}$ phenotype.

Concerning how Src family kinases participate in the generation of the inflammatory environment, our biochemical studies (Fig. 9, A–C) suggest that the Hck$^{-/-}$Fgr$^{-/-}$Lyn$^{-/-}$ mutation abrogates proximal signal transduction by activating Fcγ receptors. This is further supported by the similarities between the Hck$^{-/-}$Fgr$^{-/-}$Lyn$^{-/-}$ and FcR$\gamma^{-/-}$ mutants (Fig. 10, A–I) and the lack of rescue of the Hck$^{-/-}$Fgr$^{-/-}$Lyn$^{-/-}$ arthritis phenotype by FcR$\gamma^{-/-}$ hematopoietic cells (Fig. 10 J). As Fc receptors are also required for autoantibody-induced skin blistering disease (Sitaru et al., 2002, 2005), this may also explain the protection of Hck$^{-/-}$Fgr$^{-/-}$Lyn$^{-/-}$ mice in that model (Fig. 3, A–C).

Our results (Figs. 7–10) argue against prior assumptions that Src family kinases do not play a major role in Fc receptor signaling in myeloid cells (Lowell et al., 1996; Fitzer-Attas et al., 2000; Lowell, 2004). In case of neutrophils, Lyn appears to compensate for the lack of the other two kinases in Hck$^{-/-}$Fgr$^{-/-}$ cells; therefore, a dramatic effect is only observed in Hck$^{-/-}$Fgr$^{-/-}$Lyn$^{-/-}$ triple mutants (Fig. 7, A and B). In case of macrophages, the apparent contradiction may stem from a similar compensation by another Src family kinase (e. g. Src or Yes), or by different signals required for Fc receptor–mediated phagocytosis and responses to immobilized immune complexes.

An additional level of complexity may derive from a potential role for β_2 integrins in immune complex–induced activation of myeloid cells. In agreement with a prior study (Chen et al., 2003), we observed partial reduction of immune complex–induced functional responses of CD18$^{-/-}$ neutrophils which, however, was not nearly as pronounced as the complete defect seen in Hck$^{-/-}$Fgr$^{-/-}$Lyn$^{-/-}$ and FcR$\gamma^{-/-}$ cells (unpublished data). Analysis of CD11a$^{-/-}$ and CD11b$^{-/-}$ mice revealed that the partial reduction of immune complex–induced neutrophil responses was mediated by Mac-1 (CD11b/CD18) rather than LFA-1 (CD11a/CD18), whereas, in agreement with prior studies (Watts et al., 2005; Monach et al., 2010), in vivo arthritis was primarily mediated by LFA-1 but not Mac-1 (unpublished data). In agreement with prior reports suggesting a negative role for Mac-1 in various neutrophil- and autoantibody-mediated inflammatory diseases (Watts et al., 2005; Rosetti et al., 2012), Mac-1–deficient (CD11b$^{-/-}$) mice were even hyperresponsive in the K/B×N serum transfer model (unpublished data). Furthermore, although β_2 integrin–mediated responses are primarily mediated by Hck and Fgr (Lowell et al., 1996; Mócsai et al., 1999; Suen et al.,

1999), autoantibody-induced arthritis primarily relies on Hck and Lyn (Fig. 2). Those points together suggest that the amplification of immune complex–induced neutrophil responses by β_2 integrins (primarily Mac-1) is unlikely to substantially contribute to the in vivo arthritis defect in $Hck^{-/-}Fgr^{-/-}Lyn^{-/-}$ mice.

Collectively, our experiments have revealed a critical role for Src family kinases in various myeloid cell–mediated animal models of human disease. The role of Src family kinases was related to the immune complex–induced generation of an inflammatory microenvironment, revealing a so-far underestimated role for Src family kinases in the inflammatory response. Those results may contribute to the understanding, diagnosis, and therapy of major human diseases such as rheumatoid arthritis and inflammatory skin diseases.

MATERIALS AND METHODS

Animals. Mice homozygous for the *Hck*^{tm1Hev}, *Fgr*^{tm1Hev}, or *Lyn*^{tm1Sor} mutations (referred to as $Hck^{-/-}$, $Fgr^{-/-}$, or $Lyn^{-/-}$ mice, respectively) were described before (Lowell et al., 1994; Chan et al., 1997). Single, as well as combined double and triple knockout strains were maintained in homozygous form, except for the Hck/Lyn double mutation which was maintained in $Hck^{-/-}Lyn^{+/-}$ form due to the limited viability of $Hck^{-/-}Lyn^{-/-}$ mice (Xiao et al., 2008). It should be noted that although $Hck^{-/-}Lyn^{-/-}$ double knockout mice were of poor overall health and died within 2 mo after birth, $Hck^{-/-}Fgr^{-/-}Lyn^{-/-}$ triple knockouts were apparently healthy and bred normally in homozygous form, indicating that the severe myeloproliferation reported in $Hck^{-/-}Lyn^{-/-}$ mice (Xiao et al., 2008) is somehow mediated by the Fgr kinase.

Complete CD18-deficient (*Itgb2*$^{tm2Bay/tm2Bay}$, referred to as $CD18^{-/-}$) mice (Scharffetter-Kochanek et al., 1998) were obtained from A. Beaudet (Baylor College of Medicine, Houston, TX). CD11a-deficient (*Itgal*$^{tm1Hogg/tm1Hogg}$, referred to as $CD11a^{-/-}$) mice (Berlin-Rufenach et al., 1999) were obtained from N. Hogg (Cancer Research UK, London, UK). CD11b-deficient (*Itgam*$^{tm1Myd/tm1Myd}$, referred to as $CD11b^{-/-}$) mice (Coxon et al., 1996) were purchased from The Jackson Laboratory. FcRγ-deficient (*Fcer1g*$^{tm1Rav/tm1Rav}$, referred to as $FcR\gamma^{-/-}$) mice (Takai et al., 1994) were purchased from Taconic. Mice carrying the KRN T cell receptor transgene (Tg(TcraR28,Tcrb R28)KRNDim; Kouskoff et al., 1996) were obtained from D. Mathis and C. Benoist (Harvard Medical School, Boston, MA) and maintained in heterozygous form by mating with C57BL/6 mice.

All transgenic mice were backcrossed to the C57BL/6 genetic background for at least 6 generations. Genotyping was performed by allele-specific PCR. WT control C57BL/6 mice were purchased from Charles River or the Hungarian National Institute of Oncology. NOD mice, as well as a congenic strain carrying the CD45.1 allele on the C57BL/6 genetic background (B6.SJL-*Ptprc*^{a}), were purchased from The Jackson Laboratory. Mice were kept in individually sterile ventilated cages (Tecniplast) in a conventional facility. All animal experiments were approved by the Animal Experimentation Review Board of the Semmelweis University or the University of Pécs.

Bone marrow chimeras were generated by intravenous injection of unfractionated bone marrow cells into recipients carrying the CD45.1 allele on the C57BL/6 genetic background, which were lethally irradiated before by 11.5 Gy from a ^{137}Cs source using a Gamma-Service Medical D1 irradiator. To test the role of Hck, Fgr, and Lyn in the nonhematopoietic compartment, $Hck^{-/-}Fgr^{-/-}Lyn^{-/-}$ mice were irradiated and transplanted with CD45.1-expressing WT donor bone marrow cells. 3–6 wk after transplantation, peripheral blood samples were stained for Ly6G and CD45.2 and analyzed by flow cytometry (see below). Repopulation of the hematopoietic compartment by donor-derived cells was defined as the percentage of donor-derived cells in the Ly6G-positive granulocyte gate. Bone marrow chimeras were used 4–10 wk after the transplantation, except for $Hck^{-/-}Lyn^{-/-}$ chimeras which, due to their reported health issues (Xiao et al., 2008), were used 3–5 wk after transplantation.

Mixed bone marrow chimeras carrying $Hck^{-/-}Fgr^{-/-}Lyn^{-/-}$ and $FcR\gamma^{-/-}$ cells were generated as described above using a mixture of $Hck^{-/-}Fgr^{-/-}Lyn^{-/-}$ and $FcR\gamma^{-/-}$ donor bone marrow cells in the range of 1:3 to 3:1 ratios. The percentage of the two genotypes in the Ly6G-positive granulocyte gate in the resulting chimeras was tested by flow cytometry using an Alexa Fluor 647–conjugated antibody (clone 9E9; provided by F. Nimmerjahn, Erlangen, Germany) against mouse FcγRIV which is not expressed on $FcR\gamma^{-/-}$ neutrophils (Nimmerjahn et al., 2005). Generation and analysis of mixed bone marrow chimeras for competitive migration experiments is described below.

K/B×N serum transfer arthritis. Mice carrying the KRN T cell receptor transgene on the C57BL/6 genetic background were mated with NOD mice to obtain transgene-positive (arthritic) K/B×N and transgene-negative (nonarthritic) B×N mice (Kouskoff et al., 1996; Jakus et al., 2009). The presence of the transgene was determined by allele-specific PCR and confirmed by phenotypic assessment. Blood was taken by retro-orbital bleeding and sera from arthritic and control mice were pooled separately.

Arthritis was induced by intraperitoneal injection of 300 µl K/B×N (arthritic) or B×N (control) serum into intact mice or bone marrow chimeras, followed by daily assessment of arthritis severity for 2 wk as previously described (Jakus et al., 2009). Visible clinical signs were scored on a 0–10 scale by two investigators blinded for the origin and treatment of the mice. Ankle thickness was measured by a spring-loaded caliper (Kroeplin). For histological analysis, mice were sacrificed 7 d after serum transfer, their ankles were fixed in formalin, decalcified, embedded in paraffin, sectioned at 5 µm thickness, and stained with hematoxylin and eosin (Helyes et al., 2004). Images were captured with an inverted microscope (DMI 6000B; Leica) using a 5× objective in transmitted light mode.

To assess articular function, mice were placed on a custom-made (Charles River Hungary) wire grid, slowly flipped, and the length of time the mice held on to the grid was recorded as previously described (Jakus et al., 2009). This test was performed 3 times daily during the period of 6–12 d after the serum injection. The obtained data were combined into "holding-on curves" for each mouse.

In vivo imaging of ROS production. A luminol chemiluminescence assay was used to detect in vivo MPO activity (Gross et al., 2009). Mice were anaesthetized with 50 mg/kg pentobarbital sodium i.p. and injected i.p. with 150 mg/kg luminol sodium salt (Sigma-Aldrich) dissolved in PBS. Luminescence images were captured 10 min after the injection with an IVIS Lumina II imaging system (PerkinElmer) and processed using the Living Image software (PerkinElmer). Total radiance values (total photon flux/s) from standardized regions of interest of front and hind paws were used for quantitative analysis.

Autoantibody-induced skin blistering model. The murine model of the human autoantibody-induced blistering skin disease epidermolysis bullosa acquisita was triggered by systemic administration of antibodies against collagen VII (Sitaru et al., 2005). GST fusion proteins containing the mCVIICr fragment of mouse collagen VII were expressed in *E. coli*, purified using GST affinity columns, and used to generate polyclonal antiserum in rabbits as previously described (Csorba et al., 2010). The IgG fraction of the antiserum was prepared using a Protein G Sepharose Fast Flow affinity column chromatography (GE Healthcare) as previously described (Sitaru et al., 2005). The reactivity of the antibody preparation was tested using an ELISA with His-tagged mCVIICr fragment of murine collagen VII, as well as by indirect immunofluorescence on mouse skin sections as previously described (Csorba et al., 2010). Normal rabbit IgG (Sigma-Aldrich) was used as control.

15 mg pathogenic or control IgG per mouse was injected subcutaneously under isoflurane anesthesia on days 0 and 2, followed by 10 mg IgG/mouse on days 4, 6, and 8 (60 mg total IgG/mouse). The disease onset and progression was followed by clinical assessment and photodocumentation every two days. Scoring was based on the specific dermatological abnormalities (e.g., erythema, blister, crust) and the size of the affected skin area, with the latter determined using predefined percentages of the various areas of the skin of mice (e.g., one ear: 2.5%; snout: 5%; etc.). Antibody levels against collagen VII in blood samples at day 6 were determined by ELISA.

Reverse passive Arthus reaction. To trigger the cutaneous reverse passive Arthus reaction, WT or $Hck^{-/-}Fgr^{-/-}Lyn^{-/-}$ mice were anesthetized by 2.5% tribromoethanol (Sigma-Aldrich) in PBS and injected intradermally into the right ear, with 20 µl rabbit polyclonal anti–chicken egg albumin (Ova; Sigma-Aldrich) whole serum diluted twofold in PBS. Similarly prepared normal rabbit serum (Sigma-Aldrich) was injected into the left ears as controls. This was immediately followed by i.v. injection of 0.4 mg ovalbumin (Sigma-Aldrich). 2 h later, the mice were injected i.v. with 80 MBq ^{99m}Tc-labeled human serum albumin (prepared using the Albumon HSA ^{99m}Tc labeling kit from Medi-Radiopharma, and ^{99m}Tc-pertechnetate harvested from a Sorin/Drygen generator from Izotóp Intézet). After two more hours, mice were anesthetized with 10% urethan and the distribution of the radioactivity was detected using a NanoSPECT/CT Silver Upgrade SPECT/CT system (Mediso) along with a reference CT scan. Data were processed using the Fusion (Mediso) and VivoQuant (inviCRO) software. The radioactivity of the ears was normalized to that of the entire head area.

In vivo analysis of myeloid cell migration. In case of the K/B×N serum transfer model, the ankle or front paw area was flushed with 1 ml PBS supplemented with 10 mM EDTA (pH 7.5) and 20 mM HEPES (pH 7.4; Sigma) on day 4 to obtain a sample of synovial infiltrate. In case of the autoantibody-induced skin blistering model, the skin of the buccal area (which was most consistently affected by disease development) was isolated on day 7, minced, and digested with 28 U/ml Liberase and 10 mg/ml DNase I (both from Roche) in Ca^{2+} and Mg^{2+}-containing Hank's balanced salt solution (HBSS; Invitrogen) supplemented with 20 mM Hepes, pH 7.4, for 1 h at 37°C with thorough stirring. The number and distribution of the myeloid cells in the resulting suspension was then determined by flow cytometry. Myeloid cell types were identified based on their typical forward and side scatter characteristics, as well as by positive staining of neutrophils for Ly6G (clone 1A8; BD), or positive staining of monocytes/macrophages for F4/80 (clone A3-1; AbD Serotec) or CD11b (clone M1/70; BD) within the Ly6G-negative gate.

A competitive migration assay in mixed bone marrow chimeras (Jakus et al., 2009) was also used to assess in vivo migration of myeloid cells. To this end, WT (C57BL/6), $Hck^{-/-}Fgr^{-/-}Lyn^{-/-}$, $CD18^{-/-}$, or $FcR\gamma^{-/-}$ bone marrow cells (all carrying the CD45.2 allele) were mixed at varying ratios ranging from 1:4 to 4:1 with bone marrow cells from congenic mice expressing CD45.1 on the C57BL/6 genetic background. This mixed cell suspension was injected intravenously into lethally irradiated CD45.1-expressing recipient mice, giving rise to mixed bone marrow chimeras carrying CD45.2-expressing WT, $CD18^{-/-}$, $Hck^{-/-}Fgr^{-/-}Lyn^{-/-}$, or $FcR\gamma^{-/-}$, along with CD45.1-expressing WT hematopoietic cells within the same animals. 5–8 wk after transplantation, the chimeras were subjected to K/B×N serum transfer arthritis and their synovial infiltrates were prepared as described above. The percentage of CD45.2-expressing cells within the above defined neutrophil and monocyte/macrophage gates from the synovial infiltrate and from peripheral blood samples were analyzed by flow cytometry as described above, with an additional staining for CD45.2 (clone 104; BD).

Relative migration (accumulation) of the CD45.2-positive neutrophils or monocytes/macrophages (relative to the CD45.1-expressing WT cells) was calculated as follows:

$$\text{relative migration} = \frac{\left(\frac{\text{percentage of CD45.2 cells in synovial infiltrate}}{\text{percentage of CD45.2 cells in blood}}\right)}{\left(\frac{\text{percentage of CD45.1 cells in synovial infiltrate}}{\text{percentage of CD45.1 cells in blood}}\right)}$$

Isolation and activation of neutrophils, monocytes, and macrophages. Mouse neutrophils were isolated from the bone marrow of the femurs and tibias of intact mice by hypotonic lysis followed by Percoll (GE Healthcare) gradient centrifugation using sterile and endotoxin-free reagents as previously described (Mócsai et al., 2003). Cells were kept at room temperature in Ca^{2+}- and Mg^{2+}-free medium until use (usually less than 30 min) and prewarmed to 37°C before activation. Neutrophil assays were performed at 37°C in HBSS supplemented with 20 mM Hepes, pH 7.4.

Mouse bone marrow-derived macrophages were obtained by culturing bone marrow cells from intact mice in α-MEM (Sigma) complemented with 10% FCS (Invitrogen), 2 mM L-glutamine, antibiotics, 10 mM HEPES (all from Sigma-Aldrich), and 10% conditioned medium from CMG 14–12 cells as a source of recombinant murine M-CSF (Kertész et al., 2012) for 8–10 d on bacterial Petri dishes with media changes every 2–3 d. Cells were suspended by 5 mM EDTA, washed and serum-starved for 2 h before the experiments.

Mouse monocytes were isolated from the bone marrow of femurs and tibias of intact mice using a CD115 MicroBead kit (Miltenyi Biotec), followed by magnetic separation on LS columns (Miltenyi Biotec) according to the manufacturer's instructions. Sample purity was >95% as tested by flow cytometry using F4/80 and Ly6G staining. In vitro monocyte assays were performed in HBSS supplemented with 20 mM Hepes, pH 7.4. Cells were kept at 4°C throughout the separation and were prewarmed to 37°C before the assay.

To obtain immobilized immune complex–coated surfaces, human serum albumin (HSA; Sigma-Aldrich) was either bound directly to regular or luminometric Nunc MaxiSorp F96 (Thermo Fisher Scientific) plates or covalently linked to poly-L-lysine–coated 6-cm tissue culture dishes and then treated with anti-HSA IgG (Sigma-Aldrich) as previously described (Jakus et al., 2008). For the analysis of proinflammatory mediator release, 100 µl aliquots of 4×10^6/ml neutrophils or 500 µl aliquots of 3×10^6/ml macrophages suspended in HBSS supplemented with 20 mM Hepes, pH 7.4, were plated on immobilized immune complex surfaces in 96-well ELISA plates or 24-well tissue culture plates, respectively, stimulated for 6 or 24 h, respectively, and the inflammatory mediator concentration of the supernatant was determined as described below. For the analysis of LTB_4 production, 100 µl aliquots of 4×10^6/ml neutrophils or 500 µl aliquots of 3×10^6/ml macrophages suspended in DMEM (Sigma-Aldrich) were plated on immobilized immune complex surfaces in 96-well ELISA plates or 24-well tissue culture plates, respectively, for 1 h and the LTB_4 concentration of the cell-free supernatant was measured as described below. Superoxide release by neutrophils was followed by a cytochrome *c* reduction test from 100 µl aliquots of 4×10^6/ml cells plated on immune complex–coated surfaces in 96-well ELISA plates as previously described (Németh et al., 2010). To test ROS production by macrophages, 100 µl aliquots of 3×10^6/ml cells were plated on immune complex–coated surfaces in 96-well luminometric ELISA plates in the presence of 50 µg/ml lucigenin (Sigma-Aldrich), and the chemiluminescence of the samples was followed by a luminometer (Mithras LB 940; Berthold).

In vitro migration of neutrophils and monocytes was tested using a Transwell (Corning) assay with inserts of 3 µm pore size coated with human fibrinogen as previously described (Jakus et al., 2009). 100 ng/ml MIP-2, 100 ng/ml MCP-1, 100 ng/ml MIP-1α (all from PeproTech) or 50 ng/ml LTB_4 (Santa Cruz Biotechnology, Inc.) was used as chemoattractants. Transmigrated cells were counted using a Neubauer chamber (monocytes) or measured by an acid phosphatase assay (neutrophils; Jakus et al., 2009).

To test neutrophil adhesion to ICAM-1, 96-well ELISA plates were coated with 10 µg/ml recombinant mouse ICAM-1 (Fc chimera; R&D Systems) in 50 mM carbonate buffer, pH 9.6, and blocked with 10% FCS (Invitrogen). 4×10^6/ml neutrophils were plated on the ICAM-1–coated surface, stimulated with 50 ng/ml mouse TNF (PeproTech), and incubated for 1 h. The adhesion of the cells was then determined using an acid phosphatase assay (Jakus et al., 2009).

Analysis of inflammatory mediators. The release of inflammatory mediators was tested from the cell-free supernatants of synovial infiltrates or of in vitro stimulated neutrophils or macrophages. Semiquantitative analysis of the level of inflammation-related chemokines and cytokines was performed using a mouse cytokine antibody array kit (Panel A from R&D Systems) according to the manufacturer's instructions and quantified using densitometry of x-ray films. The levels of IL-1β, KC, MCP-1, MIP-1α, and MIP-2, as well as of the lipid mediator LTB_4, were further tested by commercial ELISA kits (R&D Systems) according to the manufacturer's instructions.

Biochemical studies. For analysis of intracellular signaling, 8×10^6 neutrophils in 1 ml assay buffer were plated on immune complex-covered 6-cm tissue culture dishes and incubated for 10 min at 37°C. The reaction was stopped on ice and the cells (adherent and nonadherent combined) were lysed in 100 mM NaCl, 30 mM Na-Hepes, pH 7.4, 20 mM NaF, 1 mM Na-EGTA, 1% Triton X-100, and 1 mM benzamidine, freshly supplemented with 0.1 U/ml Aprotinin, 1:100 Mammalian Protease Inhibitor Cocktail, 1:100 Phosphatase Inhibitor Cocktail 2, and 1 mM PMSF (all from Sigma-Aldrich). After removal of insoluble material, lysates were either boiled in sample buffer or processed for immunoprecipitation or GST pulldown assays. Immunoprecipitation of Syk was performed using a rabbit polyclonal anti-murine Syk antiserum (Turner et al., 1995; provided by V. Tybulewicz, National Institute for Medical Research, London, UK), followed by capturing with a combination of Protein A–Sepharose (Invitrogen) and Protein G–Agarose (Invitrogen) as previously described (Mócsai et al., 2000, 2004, 2006). GST-Syk$(SH2)_2$ pulldown experiments were performed as previously described (Mócsai et al., 2004, 2006).

Whole cell lysates, immunoprecipitates, and GST-Syk$(SH2)_2$ pulldown samples were run on SDS-PAGE and immunoblotted using antibodies against phosphotyrosine (4G10; Millipore), the FcRγ-chain (Millipore), or Syk (using the precipitating antibody), followed by peroxidase-labeled secondary antibodies (GE Healthcare). The signal was developed using the ECL system (GE Healthcare) and exposed to x-ray film.

Presentation of the data and statistical analysis. Experiments were performed the indicated number of times. Quantitative graphs show mean and SEM from all independent in vitro experiments or from all individual mice from the indicated number of experiments. In case of kinetic assays, the area under the curve (AUC) calculated after subtraction of the zero time point values has been used for further calculations and analyses. For the determination of statistical significance, the response of each genotype was calculated by subtracting the control values from that of the stimulated samples, followed by normalization to the WT response within each experiment. A two-tailed Student's *t* test with unequal variance was then performed on all normalized samples to determine whether the response in a given mutant strain was statistically different from that in the WT samples (indicated by p-values in the text). P-values <0.05 were considered statistically significant.

Online supplemental material. Table S1 includes the densitometric analysis of mouse cytokine arrays. Online supplemental material is available at http://www.jem.org/cgi/content/full/jem.20132496/DC1.

We thank Anna Tóth, Janka Csepregi, and Orsolya Kása for expert technical assistance; Bálint Balázs, Krisztián Szigeti, and Domokos Máthé for help with the NanoSPECT/CT analysis; Kinga Csorba and Mayson Mustafa for generating collagen VII antibodies; Gábor Bánhegyi for access to equipment; Diane Mathis, Christophe Benoist, Arthur Beaudet, and Nancy Hogg for transgenic animals; and Victor Tybulewicz and Falk Nimmerjahn for antibodies.

This work was supported by the European Research Council (Starting Independent Investigator Award no. 206283 to A. Mócsai), the European Union's FP7 Cooperation Program (TARKINAID project no. 282095 to A. Mócsai and C. Sitaru), the Lendület program of the Hungarian Academy of Sciences (LP2013-66/2013 to A. Mócsai and LP2014-4/2014 to Z. Jakus), and the Hungarian National Development Agency (SROP-4.2.2.A-11/1/KONV-2012-0024 to Z. Helyes). The NanoSPECT/CT studies were performed in the Nanobiotechnology and In Vivo Imaging Center jointly operated by Semmelweis University and CROmed Ltd. A. Mócsai was a recipient of a Wellcome Trust International Senior Research Fellowship (grant no. 087782). K. Futosi was a recipient of a Hungarian National Excellence Program (TÁMOP 4.2.4. A/1-11-1-2012-0001) research fellowship co-funded by the EU's European Social Fund.

The authors declare no competing financial interests.

Author contributions: M. Kovács, T. Németh, Z. Jakus, K. Futosi, and A. Mócsai designed the majority of the experiments. M. Kovács, T. Németh, and K. Futosi performed the majority of the experiments. Z. Jakus and A. Mócsai initiated the study. C. Sitaru participated in the design and execution of the skin blistering studies. E. Simon participated in the arthritis experiments. B. Botz and Z. Helyes participated in the design and execution of the in vivo MPO assays and the histological studies. M. Kovács, T. Németh, Z. Jakus, C. Sitaru, K. Futosi, B. Botz, Z. Helyes and A. Mócsai analyzed and interpreted the data. C.A. Lowell provided experimental tools and gave scientific advice. M. Kovács and A. Mócsai wrote the manuscript. A. Mócsai supervised the project.

Submitted: 2 December 2013
Accepted: 15 August 2014

REFERENCES

Berlin-Rufenach, C., F. Otto, M. Mathies, J. Westermann, M.J. Owen, A. Hamann, and N. Hogg. 1999. Lymphocyte migration in lymphocyte function-associated antigen (LFA)-1-deficient mice. *J. Exp. Med.* 189:1467–1478. http://dx.doi.org/10.1084/jem.189.9.1467

Bruhns, P. 2012. Properties of mouse and human IgG receptors and their contribution to disease models. *Blood*. 119:5640–5649. http://dx.doi.org/10.1182/blood-2012-01-380121

Chan, V.W., F. Meng, P. Soriano, A.L. DeFranco, and C.A. Lowell. 1997. Characterization of the B lymphocyte populations in Lyn-deficient mice and the role of Lyn in signal initiation and down-regulation. *Immunity*. 7:69–81. http://dx.doi.org/10.1016/S1074-7613(00)80511-7

Chen, H., A. Mócsai, H. Zhang, R.X. Ding, J.H. Morisaki, M. White, J.M. Rothfork, P. Heiser, E. Colucci-Guyon, C.A. Lowell, et al. 2003. Role for plastin in host defense distinguishes integrin signaling from cell adhesion and spreading. *Immunity*. 19:95–104. http://dx.doi.org/10.1016/S1074-7613(03)00172-9

Chen, M., B.K. Lam, Y. Kanaoka, P.A. Nigrovic, L.P. Audoly, K.F. Austen, and D.M. Lee. 2006. Neutrophil-derived leukotriene B_4 is required for inflammatory arthritis. *J. Exp. Med.* 203:837–842. http://dx.doi.org/10.1084/jem.20052371

Chen, Z., K. Oeser, W. Baum, D. Voehringer, G. Schett, and A. Bozec. 2014. Induction of TH2 cells and eosinophil by infection with *nippostrongylus brasiliensis* protects against rheumatoid arthritis. *Ann. Rheum. Dis.* 73:A72. http://dx.doi.org/10.1136/annrheumdis-2013-205124.164

Chiriac, M.T., J. Roesler, A. Sindrilaru, K. Scharffetter-Kochanek, D. Zillikens, and C. Sitaru. 2007. NADPH oxidase is required for neutrophil-dependent autoantibody-induced tissue damage. *J. Pathol.* 212:56–65. http://dx.doi.org/10.1002/path.2157

Chou, R.C., N.D. Kim, C.D. Sadik, E. Seung, Y. Lan, M.H. Byrne, B. Haribabu, Y. Iwakura, and A.D. Luster. 2010. Lipid-cytokine-chemokine cascade drives neutrophil recruitment in a murine model of inflammatory arthritis. *Immunity*. 33:266–278. http://dx.doi.org/10.1016/j.immuni.2010.07.018

Corr, M., and B. Crain. 2002. The role of FcγR signaling in the K/B x N serum transfer model of arthritis. *J. Immunol.* 169:6604–6609. http://dx.doi.org/10.4049/jimmunol.169.11.6604

Coxon, A., P. Rieu, F.J. Barkalow, S. Askari, A.H. Sharpe, U.H. von Andrian, M.A. Arnaout, and T.N. Mayadas. 1996. A novel role for the β2 integrin CD11b/CD18 in neutrophil apoptosis: a homeostatic mechanism in inflammation. *Immunity*. 5:653–666. http://dx.doi.org/10.1016/S1074-7613(00)80278-2

Csorba, K., A. Sesarman, E. Oswald, V. Feldrihan, A. Fritsch, T. Hashimoto, and C. Sitaru. 2010. Cross-reactivity of autoantibodies from patients with epidermolysis bullosa acquisita with murine collagen VII. *Cell. Mol. Life Sci.* 67:1343–1351. http://dx.doi.org/10.1007/s00018-009-0256-3

Deshmane, S.L., S. Kremlev, S. Amini, and B.E. Sawaya. 2009. Monocyte chemoattractant protein-1 (MCP-1): an overview. *J. Interferon Cytokine Res.* 29:313–326. http://dx.doi.org/10.1089/jir.2008.0027

Fagerholm, S., T.J. Hilden, and C.G. Gahmberg. 2002. Lck tyrosine kinase is important for activation of the CD11a/CD18-integrins in human T lymphocytes. *Eur. J. Immunol.* 32:1670–1678. http://dx.doi.org/10.1002/1521-4141(200206)32:6<1670::AID-IMMU1670>3.0.CO;2-M

Falanga, Y.T., N.S. Chaimowitz, N. Charles, F.D. Finkelman, N.A. Pullen, S. Barbour, K. Dholaria, T. Faber, M. Kolawole, B. Huang, et al. 2012. Lyn but not Fyn kinase controls IgG-mediated systemic anaphylaxis. *J. Immunol.* 188:4360–4368. http://dx.doi.org/10.4049/jimmunol.1003223

Feigelson, S.W., V. Grabovsky, E. Winter, L.L. Chen, R.B. Pepinsky, T. Yednock, D. Yablonski, R. Lobb, and R. Alon. 2001. The Src kinase $p56^{(lck)}$ up-regulates VLA-4 integrin affinity. Implications for rapid spontaneous and chemokine-triggered T cell adhesion to VCAM-1 and fibronectin. *J. Biol. Chem.* 276:13891–13901.

Feyerabend, T.B., A. Weiser, A. Tietz, M. Stassen, N. Harris, M. Kopf, P. Radermacher, P. Möller, C. Benoist, D. Mathis, et al. 2011. Cre-mediated cell ablation contests mast cell contribution in models of antibody- and T cell-mediated autoimmunity. *Immunity*. 35:832–844. http://dx.doi.org/10.1016/j.immuni.2011.09.015

Fitzer-Attas, C.J., M. Lowry, M.T. Crowley, A.J. Finn, F. Meng, A.L. DeFranco, and C.A. Lowell. 2000. Fcgamma receptor-mediated phagocytosis in macrophages lacking the Src family tyrosine kinases Hck, Fgr, and Lyn. *J. Exp. Med.* 191:669–682. http://dx.doi.org/10.1084/jem.191.4.669

Fumagalli, L., H. Zhang, A. Baruzzi, C.A. Lowell, and G. Berton. 2007. The Src family kinases Hck and Fgr regulate neutrophil responses to N-formyl-methionyl-leucyl-phenylalanine. *J. Immunol.* 178:3874–3885. http://dx.doi.org/10.4049/jimmunol.178.6.3874

Futosi, K., T. Németh, R. Pick, T. Vántus, B. Walzog, and A. Mócsai. 2012. Dasatinib inhibits proinflammatory functions of mature human neutrophils. *Blood*. 119:4981–4991. http://dx.doi.org/10.1182/blood-2011-07-369041

Giagulli, C., L. Ottoboni, E. Caveggion, B. Rossi, C. Lowell, G. Constantin, C. Laudanna, and G. Berton. 2006. The Src family kinases Hck and Fgr are dispensable for inside-out, chemoattractant-induced signaling regulating β_2 integrin affinity and valency in neutrophils, but are required for β_2 integrin-mediated outside-in signaling involved in sustained adhesion. *J. Immunol.* 177:604–611. http://dx.doi.org/10.4049/jimmunol.177.1.604

Gomez, G., C. Gonzalez-Espinosa, S. Odom, G. Baez, M.E. Cid, J.J. Ryan, and J. Rivera. 2005. Impaired FcεRI-dependent gene expression and defective eicosanoid and cytokine production as a consequence of Fyn deficiency in mast cells. *J. Immunol.* 175:7602–7610. http://dx.doi.org/10.4049/jimmunol.175.11.7602

Gross, S., S.T. Gammon, B.L. Moss, D. Rauch, J. Harding, J.W. Heinecke, L. Ratner, and D. Piwnica-Worms. 2009. Bioluminescence imaging of myeloperoxidase activity in vivo. *Nat. Med.* 15:455–461. http://dx.doi.org/10.1038/nm.1886

Helyes, Z., A. Szabó, J. Németh, B. Jakab, E. Pintér, A. Bánvölgyi, L. Kereskai, G. Kéri, and J. Szolcsányi. 2004. Antiinflammatory and analgesic effects of somatostatin released from capsaicin-sensitive sensory nerve terminals in a Freund's adjuvant-induced chronic arthritis model in the rat. *Arthritis Rheum.* 50:1677–1685. http://dx.doi.org/10.1002/art.20184

Hernandez-Hansen, V., A.J. Smith, Z. Surviladze, A. Chigaev, T. Mazel, J. Kalesnikoff, C.A. Lowell, G. Krystal, L.A. Sklar, B.S. Wilson, and J.M. Oliver. 2004. Dysregulated FcεRI signaling and altered Fyn and SHIP activities in Lyn-deficient mast cells. *J. Immunol.* 173:100–112. http://dx.doi.org/10.4049/jimmunol.173.1.100

Hibbs, M.L., D.M. Tarlinton, J. Armes, D. Grail, G. Hodgson, R. Maglitto, S.A. Stacker, and A.R. Dunn. 1995. Multiple defects in the immune system of Lyn-deficient mice, culminating in autoimmune disease. *Cell.* 83:301–311. http://dx.doi.org/10.1016/0092-8674(95)90171-X

Hirahashi, J., D. Mekala, J. Van Ziffle, L. Xiao, S. Saffaripour, D.D. Wagner, S.D. Shapiro, C. Lowell, and T.N. Mayadas. 2006. Mac-1 signaling via Src-family and Syk kinases results in elastase-dependent thrombohemorrhagic vasculopathy. *Immunity*. 25:271–283. http://dx.doi.org/10.1016/j.immuni.2006.05.014

Jacobs, J.P., A. Ortiz-Lopez, J.J. Campbell, C.J. Gerard, D. Mathis, and C. Benoist. 2010. Deficiency of CXCR2, but not other chemokine receptors, attenuates autoantibody-mediated arthritis in a murine model. *Arthritis Rheum.* 62:1921–1932.

Jakus, Z., T. Németh, J.S. Verbeek, and A. Mócsai. 2008. Critical but overlapping role of FcγRIII and FcγRIV in activation of murine neutrophils by immobilized immune complexes. *J. Immunol.* 180:618–629. http://dx.doi.org/10.4049/jimmunol.180.1.618

Jakus, Z., E. Simon, D. Frommhold, M. Sperandio, and A. Mócsai. 2009. Critical role of phospholipase Cγ2 in integrin and Fc receptor-mediated neutrophil functions and the effector phase of autoimmune arthritis. *J. Exp. Med.* 206:577–593. http://dx.doi.org/10.1084/jem.20081859

Ji, H., K. Ohmura, U. Mahmood, D.M. Lee, F.M. Hofhuis, S.A. Boackle, K. Takahashi, V.M. Holers, M. Walport, C. Gerard, et al. 2002. Arthritis critically dependent on innate immune system players. *Immunity*. 16:157–168. http://dx.doi.org/10.1016/S1074-7613(02)00275-3

Kawakami, Y., J. Kitaura, A.B. Satterthwaite, R.M. Kato, K. Asai, S.E. Hartman, M. Maeda-Yamamoto, C.A. Lowell, D.J. Rawlings, O.N. Witte, and T. Kawakami. 2000. Redundant and opposing functions of two tyrosine kinases, Btk and Lyn, in mast cell activation. *J. Immunol.* 165:1210–1219. http://dx.doi.org/10.4049/jimmunol.165.3.1210

Kertész, Z., D. Győri, S. Körmendi, T. Fekete, K. Kis-Tóth, Z. Jakus, G. Schett, E. Rajnavölgyi, C. Dobó-Nagy, and A. Mócsai. 2012. Phospholipase Cγ2 is required for basal but not oestrogen deficiency-induced bone resorption. *Eur. J. Clin. Invest.* 42:49–60. http://dx.doi.org/10.1111/j.1365-2362.2011.02556.x

Kim, N.D., R.C. Chou, E. Seung, A.M. Tager, and A.D. Luster. 2006. A unique requirement for the leukotriene B_4 receptor BLT1 for neutrophil recruitment in inflammatory arthritis. *J. Exp. Med.* 203:829–835. http://dx.doi.org/10.1084/jem.20052349

Kim, L.C., L. Song, and E.B. Haura. 2009. Src kinases as therapeutic targets for cancer. *Nat. Rev. Clin. Oncol.* 6:587–595. http://dx.doi.org/10.1038/nrclinonc.2009.129

Korganow, A.S., H. Ji, S. Mangialaio, V. Duchatelle, R. Pelanda, T. Martin, C. Degott, H. Kikutani, K. Rajewsky, J.L. Pasquali, et al. 1999. From systemic T cell self-reactivity to organ-specific autoimmune disease via immunoglobulins. *Immunity*. 10:451–461. http://dx.doi.org/10.1016/S1074-7613(00)80045-X

Kouskoff, V., A.S. Korganow, V. Duchatelle, C. Degott, C. Benoist, and D. Mathis. 1996. Organ-specific disease provoked by systemic autoimmunity. *Cell*. 87:811–822. http://dx.doi.org/10.1016/S0092-8674(00)81989-3

Lämmermann, T., B.L. Bader, S.J. Monkley, T. Worbs, R. Wedlich-Söldner, K. Hirsch, M. Keller, R. Förster, D.R. Critchley, R. Fässler, and M. Sixt. 2008. Rapid leukocyte migration by integrin-independent flowing and squeezing. *Nature*. 453:51–55. http://dx.doi.org/10.1038/nature06887

Lee, D.M., D.S. Friend, M.F. Gurish, C. Benoist, D. Mathis, and M.B. Brenner. 2002. Mast cells: a cellular link between autoantibodies and inflammatory arthritis. *Science*. 297:1689–1692. http://dx.doi.org/10.1126/science.1073176

Liu, Z., L.A. Diaz, J.L. Troy, A.F. Taylor, D.J. Emery, J.A. Fairley, and G.J. Giudice. 1993. A passive transfer model of the organ-specific autoimmune disease, bullous pemphigoid, using antibodies generated against the hemidesmosomal antigen, BP180. *J. Clin. Invest.* 92:2480–2488. http://dx.doi.org/10.1172/JCI116856

Liu, Z., S.D. Shapiro, X. Zhou, S.S. Twining, R.M. Senior, G.J. Giudice, J.A. Fairley, and L.A. Diaz. 2000. A critical role for neutrophil elastase in experimental bullous pemphigoid. *J. Clin. Invest.* 105:113–123. http://dx.doi.org/10.1172/JCI3693

Liu, Z., M. Zhao, N. Li, L.A. Diaz, and T.N. Mayadas. 2006. Differential roles for β_2 integrins in experimental autoimmune bullous pemphigoid. *Blood*. 107:1063–1069. http://dx.doi.org/10.1182/blood-2005-08-3123

Lowell, C.A. 2004. Src-family kinases: rheostats of immune cell signaling. *Mol. Immunol.* 41:631–643. http://dx.doi.org/10.1016/j.molimm.2004.04.010

Lowell, C.A., and G. Berton. 1998. Resistance to endotoxic shock and reduced neutrophil migration in mice deficient for the Src-family kinases Hck and Fgr. *Proc. Natl. Acad. Sci. USA*. 95:7580–7584. http://dx.doi.org/10.1073/pnas.95.13.7580

Lowell, C.A., P. Soriano, and H.E. Varmus. 1994. Functional overlap in the src gene family: inactivation of hck and fgr impairs natural immunity. *Genes Dev.* 8:387–398. http://dx.doi.org/10.1101/gad.8.4.387

Lowell, C.A., L. Fumagalli, and G. Berton. 1996. Deficiency of Src family kinases $p59/61^{hck}$ and $p58^{c\text{-}fgr}$ results in defective adhesion-dependent neutrophil functions. *J. Cell Biol.* 133:895–910. http://dx.doi.org/10.1083/jcb.133.4.895

Meng, F., and C.A. Lowell. 1998. A β_1 integrin signaling pathway involving Src-family kinases, Cbl and PI-3 kinase is required for macrophage spreading and migration. *EMBO J.* 17:4391–4403. http://dx.doi.org/10.1093/emboj/17.15.4391

Mizgerd, J.P., H. Kubo, G.J. Kutkoski, S.D. Bhagwan, K. Scharffetter-Kochanek, A.L. Beaudet, and C.M. Doerschuk. 1997. Neutrophil emigration in the skin, lungs, and peritoneum: different requirements for CD11/CD18 revealed by CD18-deficient mice. *J. Exp. Med.* 186:1357–1364. http://dx.doi.org/10.1084/jem.186.8.1357

Mócsai, A., E. Ligeti, C.A. Lowell, and G. Berton. 1999. Adhesion-dependent degranulation of neutrophils requires the Src family kinases Fgr and Hck. *J. Immunol.* 162:1120–1126.

Mócsai, A., Z. Jakus, T. Vántus, G. Berton, C.A. Lowell, and E. Ligeti. 2000. Kinase pathways in chemoattractant-induced degranulation of neutrophils: the

role of p38 mitogen-activated protein kinase activated by Src family kinases. *J. Immunol.* 164:4321–4331. http://dx.doi.org/10.4049/jimmunol.164.8.4321

Mócsai, A., M. Zhou, F. Meng, V.L. Tybulewicz, and C.A. Lowell. 2002. Syk is required for integrin signaling in neutrophils. *Immunity*. 16:547–558. http://dx.doi.org/10.1016/S1074-7613(02)00303-5

Mócsai, A., H. Zhang, Z. Jakus, J. Kitaura, T. Kawakami, and C.A. Lowell. 2003. G-protein-coupled receptor signaling in Syk-deficient neutrophils and mast cells. *Blood*. 101:4155–4163. http://dx.doi.org/10.1182/blood-2002-07-2346

Mócsai, A., M.B. Humphrey, J.A. Van Ziffle, Y. Hu, A. Burghardt, S.C. Spusta, S. Majumdar, L.L. Lanier, C.A. Lowell, and M.C. Nakamura. 2004. The immunomodulatory adapter proteins DAP12 and Fc receptor γ-chain (FcRγ) regulate development of functional osteoclasts through the Syk tyrosine kinase. *Proc. Natl. Acad. Sci. USA*. 101:6158–6163. http://dx.doi.org/10.1073/pnas.0401602101

Mócsai, A., C.L. Abram, Z. Jakus, Y. Hu, L.L. Lanier, and C.A. Lowell. 2006. Integrin signaling in neutrophils and macrophages uses adaptors containing immunoreceptor tyrosine-based activation motifs. *Nat. Immunol.* 7:1326–1333. http://dx.doi.org/10.1038/ni1407

Monach, P.A., P.A. Nigrovic, M. Chen, H. Hock, D.M. Lee, C. Benoist, and D. Mathis. 2010. Neutrophils in a mouse model of autoantibody-mediated arthritis: critical producers of Fc receptor γ, the receptor for C5a, and lymphocyte function-associated antigen 1. *Arthritis Rheum.* 62:753–764. http://dx.doi.org/10.1002/art.27238

Morgan, M.M., C.M. Labno, G.A. Van Seventer, M.F. Denny, D.B. Straus, and J.K. Burkhardt. 2001. Superantigen-induced T cell:B cell conjugation is mediated by LFA-1 and requires signaling through Lck, but not ZAP-70. *J. Immunol.* 167:5708–5718. http://dx.doi.org/10.4049/jimmunol.167.10.5708

Németh, T., K. Futosi, C. Hably, M.R. Brouns, S.M. Jakob, M. Kovács, Z. Kertész, B. Walzog, J. Settleman, and A. Mócsai. 2010. Neutrophil functions and autoimmune arthritis in the absence of p190RhoGAP: generation and analysis of a novel null mutation in mice. *J. Immunol.* 185:3064–3075. http://dx.doi.org/10.4049/jimmunol.0904163

Nimmerjahn, F., P. Bruhns, K. Horiuchi, and J.V. Ravetch. 2005. FcγRIV: a novel FcR with distinct IgG subclass specificity. *Immunity*. 23:41–51. http://dx.doi.org/10.1016/j.immuni.2005.05.010

Nishizumi, H., and T. Yamamoto. 1997. Impaired tyrosine phosphorylation and Ca^{2+} mobilization, but not degranulation, in lyn-deficient bone marrow-derived mast cells. *J. Immunol.* 158:2350–2355.

Nishizumi, H., I. Taniuchi, Y. Yamanashi, D. Kitamura, D. Ilic, S. Mori, T. Watanabe, and T. Yamamoto. 1995. Impaired proliferation of peripheral B cells and indication of autoimmune disease in lyn-deficient mice. *Immunity*. 3:549–560. http://dx.doi.org/10.1016/1074-7613(95)90126-4

Nussbaum, C., A. Klinke, M. Adam, S. Baldus, and M. Sperandio. 2013. Myeloperoxidase: a leukocyte-derived protagonist of inflammation and cardiovascular disease. *Antioxid. Redox Signal.* 18:692–713. http://dx.doi.org/10.1089/ars.2012.4783

Odom, S., G. Gomez, M. Kovarova, Y. Furumoto, J.J. Ryan, H.V. Wright, C. Gonzalez-Espinosa, M.L. Hibbs, K.W. Harder, and J. Rivera. 2004. Negative regulation of immunoglobulin E-dependent allergic responses by Lyn kinase. *J. Exp. Med.* 199:1491–1502. http://dx.doi.org/10.1084/jem.20040382

Palacios, E.H., and A. Weiss. 2004. Function of the Src-family kinases, Lck and Fyn, in T-cell development and activation. *Oncogene*. 23:7990–8000. http://dx.doi.org/10.1038/sj.onc.1208074

Parravicini, V., M. Gadina, M. Kovarova, S. Odom, C. Gonzalez-Espinosa, Y. Furumoto, S. Saitoh, L.E. Samelson, J.J. O'Shea, and J. Rivera. 2002. Fyn kinase initiates complementary signals required for IgE-dependent mast cell degranulation. *Nat. Immunol.* 3:741–748.

Parsons, S.J., and J.T. Parsons. 2004. Src family kinases, key regulators of signal transduction. *Oncogene*. 23:7906–7909. http://dx.doi.org/10.1038/sj.onc.1208160

Pereira, S., M. Zhou, A. Mócsai, and C. Lowell. 2001. Resting murine neutrophils express functional α_4 integrins that signal through Src family kinases. *J. Immunol.* 166:4115–4123. http://dx.doi.org/10.4049/jimmunol.166.6.4115

Perez, O.D., D. Mitchell, G.C. Jager, and G.P. Nolan. 2004. LFA-1 signaling through p44/42 is coupled to perforin degranulation in $CD56^+CD8^+$ natural killer cells. *Blood*. 104:1083–1093. http://dx.doi.org/10.1182/blood-2003-08-2652

Playford, M.P., and M.D. Schaller. 2004. The interplay between Src and integrins in normal and tumor biology. *Oncogene*. 23:7928–7946. http://dx.doi.org/10.1038/sj.onc.1208080

Riteau, B., D.F. Barber, and E.O. Long. 2003. Vav1 phosphorylation is induced by β_2 integrin engagement on natural killer cells upstream of actin cytoskeleton and lipid raft reorganization. *J. Exp. Med.* 198:469–474. http://dx.doi.org/10.1084/jem.20021995

Rolli, V., M. Gallwitz, T. Wossning, A. Flemming, W.W. Schamel, C. Zürn, and M. Reth. 2002. Amplification of B cell antigen receptor signaling by a Syk/ITAM positive feedback loop. *Mol. Cell*. 10:1057–1069. http://dx.doi.org/10.1016/S1097-2765(02)00739-6

Rosetti, F., N. Tsuboi, K. Chen, H. Nishi, T. Ernandez, S. Sethi, K. Croce, G. Stavrakis, J. Alcocer-Varela, D. Gómez-Martin, et al. 2012. Human lupus serum induces neutrophil-mediated organ damage in mice that is enabled by Mac-1 deficiency. *J. Immunol.* 189:3714–3723. http://dx.doi.org/10.4049/jimmunol.1201594

Saijo, K., C. Schmedt, I.H. Su, H. Karasuyama, C.A. Lowell, M. Reth, T. Adachi, A. Patke, A. Santana, and A. Tarakhovsky. 2003. Essential role of Src-family protein tyrosine kinases in NF-κB activation during B cell development. *Nat. Immunol.* 4:274–279. http://dx.doi.org/10.1038/ni893

Sarantos, M.R., H. Zhang, U.Y. Schaff, N. Dixit, H.N. Hayenga, C.A. Lowell, and S.I. Simon. 2008. Transmigration of neutrophils across inflamed endothelium is signaled through LFA-1 and Src family kinase. *J. Immunol.* 181:8660–8669. http://dx.doi.org/10.4049/jimmunol.181.12.8660

Scharffetter-Kochanek, K., H. Lu, K. Norman, N. van Nood, F. Munoz, S. Grabbe, M. McArthur, I. Lorenzo, S. Kaplan, K. Ley, et al. 1998. Spontaneous skin ulceration and defective T cell function in CD18 null mice. *J. Exp. Med.* 188:119–131. http://dx.doi.org/10.1084/jem.188.1.119

Schymeinsky, J., A. Mócsai, and B. Walzog. 2007. Neutrophil activation via β_2 integrins (CD11/CD18): molecular mechanisms and clinical implications. *Thromb. Haemost.* 98:262–273.

Sitaru, C. 2007. Experimental models of epidermolysis bullosa acquisita. *Exp. Dermatol.* 16:520–531. http://dx.doi.org/10.1111/j.1600-0625.2007.00564.x

Sitaru, C., A. Kromminga, T. Hashimoto, E.B. Bröcker, and D. Zillikens. 2002. Autoantibodies to type VII collagen mediate Fcgamma-dependent neutrophil activation and induce dermal-epidermal separation in cryosections of human skin. *Am. J. Pathol.* 161:301–311. http://dx.doi.org/10.1016/S0002-9440(10)64182-X

Sitaru, C., S. Mihai, C. Otto, M.T. Chiriac, I. Hausser, B. Dotterweich, H. Saito, C. Rose, A. Ishiko, and D. Zillikens. 2005. Induction of dermal-epidermal separation in mice by passive transfer of antibodies specific to type VII collagen. *J. Clin. Invest.* 115:870–878. http://dx.doi.org/10.1172/JCI200521386

Solomon, S., N. Rajasekaran, E. Jeisy-Walder, S.B. Snapper, and H. Illges. 2005. A crucial role for macrophages in the pathology of K/B x N serum-induced arthritis. *Eur. J. Immunol.* 35:3064–3073. http://dx.doi.org/10.1002/eji.200526167

Suen, P.W., D. Ilic, E. Caveggion, G. Berton, C.H. Damsky, and C.A. Lowell. 1999. Impaired integrin-mediated signal transduction, altered cytoskeletal structure and reduced motility in Hck/Fgr deficient macrophages. *J. Cell Sci.* 112:4067–4078.

Suzuki, J., S. Yamasaki, J. Wu, G.A. Koretzky, and T. Saito. 2007. The actin cloud induced by LFA-1-mediated outside-in signals lowers the threshold for T-cell activation. *Blood*. 109:168–175. http://dx.doi.org/10.1182/blood-2005-12-020164

Takai, T., M. Li, D. Sylvestre, R. Clynes, and J.V. Ravetch. 1994. FcR γ chain deletion results in pleiotrophic effector cell defects. *Cell*. 76:519–529. http://dx.doi.org/10.1016/0092-8674(94)90115-5

Turner, M., P.J. Mee, P.S. Costello, O. Williams, A.A. Price, L.P. Duddy, M.T. Furlong, R.L. Geahlen, and V.L. Tybulewicz. 1995. Perinatal lethality and blocked B-cell development in mice lacking the tyrosine kinase Syk. *Nature*. 378:298–302. http://dx.doi.org/10.1038/378298a0

van Oers, N.S., B. Lowin-Kropf, D. Finlay, K. Connolly, and A. Weiss. 1996. αβ T cell development is abolished in mice lacking both Lck and Fyn protein tyrosine kinases. *Immunity*. 5:429–436. http://dx.doi.org/10.1016/S1074-7613(00)80499-9

Vicentini, L., P. Mazzi, E. Caveggion, S. Continolo, L. Fumagalli, J.A. Lapinet-Vera, C.A. Lowell, and G. Berton. 2002. Fgr deficiency results in defective eosinophil recruitment to the lung during allergic airway inflammation. *J. Immunol.* 168:6446–6454. http://dx.doi.org/10.4049/jimmunol.168.12.6446

Walzog, B., K. Scharffetter-Kochanek, and P. Gaehtgens. 1999. Impairment of neutrophil emigration in CD18-null mice. *Am. J. Physiol.* 276:G1125–G1130.

Watts, G.M., F.J. Beurskens, I. Martin-Padura, C.M. Ballantyne, L.B. Klickstein, M.B. Brenner, and D.M. Lee. 2005. Manifestations of inflammatory arthritis are critically dependent on LFA-1. *J. Immunol.* 174:3668–3675. http://dx.doi.org/10.4049/jimmunol.174.6.3668

Wipke, B.T., and P.M. Allen. 2001. Essential role of neutrophils in the initiation and progression of a murine model of rheumatoid arthritis. *J. Immunol.* 167:1601–1608. http://dx.doi.org/10.4049/jimmunol.167.3.1601

Xiao, W., H. Hong, Y. Kawakami, C.A. Lowell, and T. Kawakami. 2008. Regulation of myeloproliferation and M2 macrophage programming in mice by Lyn/Hck, SHIP, and Stat5. *J. Clin. Invest.* 118:924–934.

Yoo, S.K., T.W. Starnes, Q. Deng, and A. Huttenlocher. 2011. Lyn is a redox sensor that mediates leukocyte wound attraction in vivo. *Nature.* 480:109–112. http://dx.doi.org/10.1038/nature10632

Zamoyska, R., A. Basson, A. Filby, G. Legname, M. Lovatt, and B. Seddon. 2003. The influence of the src-family kinases, Lck and Fyn, on T cell differentiation, survival and activation. *Immunol. Rev.* 191:107–118. http://dx.doi.org/10.1034/j.1600-065X.2003.00015.x

Zhang, S., and D. Yu. 2012. Targeting Src family kinases in anti-cancer therapies: turning promise into triumph. *Trends Pharmacol. Sci.* 33:122–128. http://dx.doi.org/10.1016/j.tips.2011.11.002

Zhang, H., F. Meng, C.L. Chu, T. Takai, and C.A. Lowell. 2005. The Src family kinases Hck and Fgr negatively regulate neutrophil and dendritic cell chemokine signaling via PIR-B. *Immunity.* 22:235–246. http://dx.doi.org/10.1016/j.immuni.2005.01.004

Zhou, J.S., W. Xing, D.S. Friend, K.F. Austen, and H.R. Katz. 2007. Mast cell deficiency in Kit($^{W\text{-}sh}$) mice does not impair antibody-mediated arthritis. *J. Exp. Med.* 204:2797–2802. http://dx.doi.org/10.1084/jem.20071391